



TRIUMF Beam Physics Note  
TRI-BN-23-14  
July, 2023

## Envelope codes why

*R. Baartman*

*TRIUMF*

**Abstract:** The virtue of statistical techniques or “envelope” codes to calculate particle beams through transport channels and accelerators is their speed. They are orders of magnitude faster than multi-particle simulations. This enables them to be useful both in designing complex systems and in operating beamlines, synchrotrons and linear accelerators.

## Contents

<b>1</b>	<b>Two purposes</b>	<b>3</b>
<b>2</b>	<b>Why envelope codes?</b>	<b>4</b>
<b>3</b>	<b>Closed-Form Matrix Methods</b>	<b>5</b>
3.1	First order pitfall . . . . .	6
3.2	Higher order undesirable effects . . . . .	6
<b>4</b>	<b>Transport Elements</b>	<b>8</b>
4.1	Solenoid . . . . .	9
4.2	Einzel Lens . . . . .	10
4.3	Quadrupole . . . . .	13
4.3.1	Quad Match Example . . . . .	14
4.4	Dipole Bender . . . . .	18
<b>5</b>	<b>Summary of Higher Order Kick Formulas</b>	<b>19</b>
<b>6</b>	<b>Growth from mismatch</b>	<b>20</b>
<b>7</b>	<b>TRANSOPTR: Beam Transport Optimization technique</b>	<b>20</b>
7.1	Optimization Engine . . . . .	21
<b>8</b>	<b>Conclusions – non-integration cases</b>	<b>24</b>
<b>9</b>	<b>TRANSOPTR: Integration mode</b>	<b>24</b>
9.1	Statistical Approach to Beam Dynamics . . . . .	25
9.2	What is <b>F</b> ? Infinitesimal Transfer Matrix . . . . .	26

9.3	Example: Quadrupole (Hard-edge) . . . . .	28
9.4	Example: Solenoid (Hard-edge) . . . . .	28
9.5	Space Charge part of $\mathbf{F}$ . . . . .	29
9.5.1	Space Charge with <b>Uniform</b> elliptical beam . . . . .	29
9.5.2	Envelope equation . . . . .	30
9.5.3	Space Charge Envelope Equations . . . . .	31
9.5.4	Bunched beams . . . . .	31
9.6	But space charge is nonlinear... what about arbitrary bunch distributions, orientations . . . . .	32
9.7	Successfully applied to: . . . . .	34
9.7.1	Example: FNAL Booster . . . . .	34
<b>10</b>	<b>Extra dividend from use of equations of motion</b>	<b>35</b>
<b>11</b>	<b>Example: Cyclotron injection line</b>	<b>36</b>
11.1	As built (1974~2011) . . . . .	37
11.2	Bunching into a $36^\circ$ phase acceptance . . . . .	37
11.3	Strong $x$ - $y$ coupling due to axial field . . . . .	38
11.4	Strong $x$ - $y$ - $z$ coupling in the inflector . . . . .	38
11.5	inflector matrix . . . . .	39
11.6	Injection Matching Detail . . . . .	39
<b>12</b>	<b>The original sin of TRANSPORT (what are the canonical vari- ables?)</b>	<b>40</b>
<b>13</b>	<b>Linac:</b>	<b>41</b>
13.1	Potentials . . . . .	41
13.2	Infinitesimal Transfer Matrix $\mathbf{F}$ . . . . .	42

13.3 Example: ISAC DTL . . . . .	43
<b>14 RFQ:</b>	<b>46</b>
14.1 Hamiltonian Dynamics . . . . .	46
14.2 RFQ Spatial Phase . . . . .	46
14.3 The On-Axis Reference Particle . . . . .	47
14.4 Hamiltonian in $(z, P_z)$ . . . . .	48
14.5 Hamiltonian for Linear motion . . . . .	48
14.6 Implementation in TRANSOPTR . . . . .	49
14.7 TRIUMF's RFQ . . . . .	50
14.8 Comparison to PARMTEQ . . . . .	50
<b>15 Application examples</b>	<b>51</b>
15.1 elinac . . . . .	51
15.2 OLIS steering training for the Bayesian optimization . . . . .	52
15.3 MCAT . . . . .	52
<b>16 Conclusions</b>	<b>52</b>
<b>17 Acknowledgements</b>	<b>53</b>

## 1 Two purposes

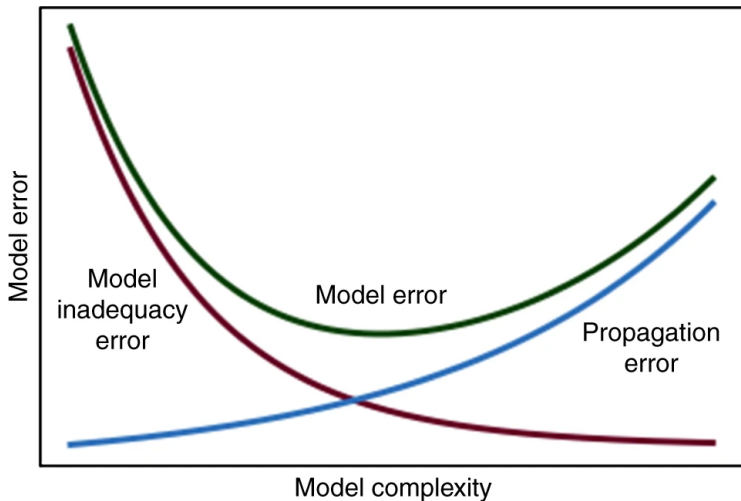
Codes are used for designing and used for tuning. Traditionally, emphasis was on former; little involvement of the beam physicists to use the actual model while commissioning was taking place. Why? Was it because there was assumed to be too many divergences between idealized model and real life? No; the basic physics is solid and simple. Real fields (on a grid) often are not needed as accuracy comes from adhering to conservation laws (canonical approach). Example: With axial symmetry, for linear description, surprisingly few points of on-axis potential are needed.

Generally what happened was that the theoretical settings were passed on to those tuning, and when those did not work, there was a lot of knobbing around. But what should happen is that the deviations between model and operation should be investigated and the model refined, so that it continues to be useful during operation.

## 2 Why envelope codes?

Why not derive accurate field maps, and shoot particles through them? Need many particles, say  $10^6$ . How many field values? Can make accurate model, but:

Often in searching through design parameter space, use a million runs. One cannot contemplate a trillion runs through a beamline just to solve this simple optimization problem. Not a good approach.



It is a fallacy that the most complete models are the most useful. It's a "can't see forest for the trees" thing: with too many details, you cannot develop any understanding of which are the important details. We want to organize particles; we don't need to know the coordinates of a billion particles.

Basic example: neither the linear, nor anything up to including third order depend strongly upon the shape of a quadrupole's fringe field; not even on the width of the fringe field. You would not know why this is, from constructing many quads with different field clamps, or from running countless cases with varying Enge coefficients.

In many cases, it is sufficient to know the beam size (in all 6 dimensions  $x_i$  for  $i = 1..6$ ). The general case is 6 sizes, 15 correlations, IOW, all second

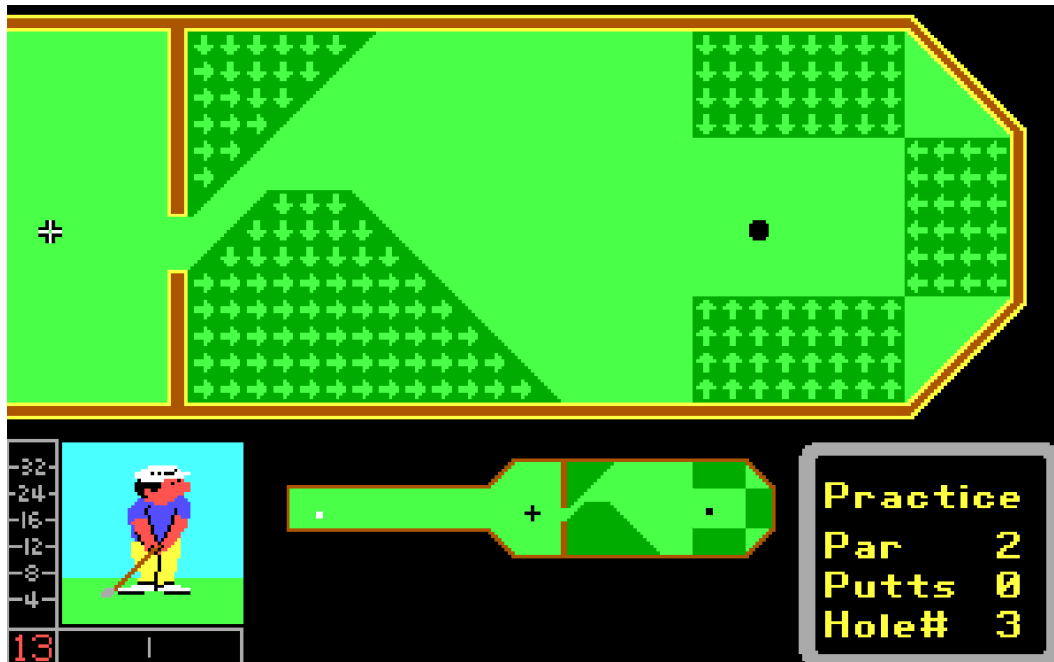
moments  $\langle x_i x_j \rangle$ . There would be 21 equations of motion of these moments rather than the  $6N$  equations where  $N = 10^6$ . So we gain five orders of magnitude in computational speed.

This was already capitalized in very early days (1960's) when computers were slow, and resulted in Brown's formulation of the  $\sigma$  matrix, and the original envelope code TRANSPORT.

### 3 Closed-Form Matrix Methods

For constant linear restoring force, matrix optics can be written in closed (matrix) form. This is the basis of early codes such as TRANSPORT. But piecewise constant fields do not satisfy Maxwell equations.

Thinking so, we make the same fundamental mistake as in this cheesy DOS game of mini-Putt. [Can you spot the problem?](#)



Interestingly, though, the perturbation from making strength a continuous function appears mostly in next higher order (cubic in the case of quadrupoles). This is called “adding fringe fields” (even COSY- $\infty$  does it) as if there's a choice. In fact **elements without fringe fields are non-physical**.

### 3.1 First order pitfall

In first order there is also an effect, that gets larger the shorter the element.

Consider that a decoupled element has a transfer matrix  $\begin{pmatrix} a & b \\ c & d \end{pmatrix}$ . Since there are only four elements and determinant is 1, only 3 are independent. Further, by time reverse symmetry,  $a = d$ . Thus there are only 2. What are they?

Effective length and effective strength, and fringe field does not seem to matter.

Effective length  $\neq$  insertion length. Moreover, effective length for  $x$  motion not the same as for  $y$  motion. Thus there are in fact four parameters; the remaining two can be called “fringe field integrals” (Wollnik[24], Irwin[1], ...).

### 3.2 Higher order undesirable effects

Since we want to design aberration-free, how can we do this with a purely linear code?

In the beginning... Slow computers, costly integration meant that analytic formulas were highly desirable. And when these were more-or-less known for the linear part, the next effort was to find the nonlinear parts. And they turned out to be very UGLY.

$$\begin{aligned}
 T_{111} &= (x|x_0^2) = && (2n-1)\beta h^3 I_{111} + \frac{1}{2} k_x^4 h I_{122} \\
 T_{112} &= (x|x_0\theta_0) = h s_x'(t) && + 2(2n-1)\beta h^3 I_{112} - k_x^2 h I_{112} \\
 T_{116} &= (x|x_0\theta) = && (2-n)h^2 I_{11} + 2(2n-1)\beta h^3 I_{116} - k_x^2 h^2 I_{122} \\
 T_{122} &= (x|\theta_0^2) = && (2n-1)\beta h^3 I_{122} + \frac{1}{2} h I_{111} \\
 T_{126} &= (x|\theta_0\theta) = && (2-n)h^2 I_{12} + 2(2n-1)\beta h^3 I_{126} + h^2 I_{112} \\
 T_{166} &= (x|\theta^2) = -h I_{10} + (2-n)h^2 I_{16} + (2n-1)\beta h^3 I_{166} + \frac{1}{2} h^3 I_{122} \\
 T_{133} &= (x|y_0^2) = && \beta h^3 I_{133} - \frac{1}{2} k_y^2 h I_{10} \\
 T_{134} &= (x|y_0\theta_0) = && 2\beta h^3 I_{134} \\
 T_{144} &= (x|\theta_0^2) = && \beta h^3 I_{144} - \frac{1}{2} h I_{10} \\
 \\ 
 T_{313} &= (y|x_0 y_0) = && + 2(\beta-n)h^3 I_{313} + k_x^2 k_y^2 h I_{324} \\
 T_{314} &= (y|x_0\theta_0) = h s_y'(t) && + 2(\beta-n)h^3 I_{314} - k_x^2 h I_{323} \\
 T_{323} &= (y|\theta_0 y_0) = && + 2(\beta-n)h^3 I_{323} - k_y^2 h I_{314} \\
 T_{324} &= (y|\theta_0\theta_0) = && + 2(\beta-n)h^3 I_{324} + h I_{313} \\
 T_{336} &= (y|y_0\theta) = k_y^2 I_{33} + 2(\beta-n)h^3 I_{336} - k_y^2 h^2 I_{324} \\
 T_{346} &= (y|\theta_0\theta) = k_y^2 I_{34} + 2(\beta-n)h^3 I_{346} + h^2 I_{323} \\
 \\ 
 T_{413} &= (y|x_0 y_0) = && 2(\beta-n)h^3 I_{413} + k_x^2 k_y^2 h I_{424} - h c_x'(t) c_y'(t) \\
 T_{414} &= (y|x_0\theta_0) = h s_y'(t) + 2(\beta-n)h^3 I_{414} - k_x^2 h I_{423} - h c_x'(t) s_y'(t) \\
 T_{423} &= (y|\theta_0 y_0) = && 2(\beta-n)h^3 I_{423} - k_y^2 h I_{414} - h s_x'(t) c_y'(t) \\
 T_{424} &= (y|\theta_0\theta_0) = && 2(\beta-n)h^3 I_{424} + h I_{413} - h s_x'(t) s_y'(t) \\
 T_{436} &= (y|y_0\theta) = k_y^2 I_{43} + 2(\beta-n)h^3 I_{436} - k_y^2 h^2 I_{424} - h d_x'(t) c_y'(t) \\
 T_{446} &= (y|\theta_0\theta) = k_y^2 I_{44} + 2(\beta-n)h^3 I_{446} + h^2 I_{423} - h d_x'(t) s_y'(t)
 \end{aligned}$$

$$\begin{aligned}
 I_{111} &= \int_0^1 c_x^2(r) G_x(r, \tau) dr = \frac{1}{3} \left( s_x^2(0) + \frac{d_x^2(0)}{h} \right) & I_{158} &= \int_0^1 d_x^2(r) G_x(r, \tau) dr = \frac{h^-}{k_x^2} \left( I_{10} - 2I_{11} + I_{111} \right) = \frac{h^-}{k_x^2} \left[ \frac{4}{3} \left( \frac{-x^{3/2}}{h} \right) + \frac{1}{3} s_x^2(0) - ts_x(0) \right] \\
 I_{112} &= \int_0^1 c_x(r) s_x(r) G_x(r, \tau) dr = \frac{1}{3} s_x(0) \left( \frac{d_x(0)}{h} \right) & I_{133} &= \int_0^1 c_y^2(r) G_x(r, \tau) dr = \left( \frac{d_x(0)}{h} \right) - \left( \frac{k_y^2}{k_x^2 - 4k_y^2} \right) \left( s_y^2(0) - 2 \frac{d_y(0)}{h} \right) = I_{10} - k_y^2 I_{144} = I_{10} - k_y^2 I_{144} \\
 I_{116} &= \int_0^1 c_x(r) d_x(r) G_x(r, \tau) dr = \frac{h}{k_x^2} \left( I_{11} - I_{111} \right) - \frac{h}{k_x^2} \left[ \frac{1}{2} s_x(0) - \frac{1}{3} \left( s_x^2(0) + \frac{d_x^2(0)}{h} \right) \right] & I_{134} &= \int_0^1 c_y(r) s_y(r) G_x(r, \tau) dr = \frac{1}{k_x^2 - 4k_y^2} \left( s_y(0) c_y(0) - s_y(0) \right) \\
 I_{122} &= \int_0^1 s_x^2(r) G_x(r, \tau) dr = \frac{1}{k_x^2} \left( I_{10} - I_{111} \right) - \frac{1}{3k_x^2} \left( 2 \frac{d_x^2(0)}{h} - s_x^2(0) \right) & I_{144} &= \int_0^1 s_y^2(r) G_x(r, \tau) dr = \frac{1}{k_x^2 - 4k_y^2} \left( s_y^2(0) - 2 \frac{d_y(0)}{h} \right) \\
 I_{126} &= \int_0^1 s_x(r) d_x(r) G_x(r, \tau) dr = \frac{h}{k_x^2} \left( I_{12} - I_{112} \right) - \frac{h}{k_x^2} \left[ \frac{1}{2k_x^2} \left( s_x(0) + d_x(0) \right) - \frac{1}{3} s_x(0) \left( \frac{d_x(0)}{h} \right) \right] - \frac{h}{6k_x^4} \left[ s_x(0) + 2s_x(0)c_x(0) - 3d_x(0) \right]
 \end{aligned}$$

...and this is only second order. The quadrupole aberrations start at third order.

Brilliantly, Martin Berz[2] devised an automatic differentiation scheme that could get these higher order matrix elements to any order. This vastly minimizes coding errors. But they were costly to calculate, so for example optimizing a beamline (minimizing aberrations) including quad lengths, strengths, apertures and separations proves to be impractical. Moreover, one had to give precisely the six Enge coefficients for any quads. (And they are not known since not yet built.) But there is an easier way. And the hint is that hardly anyone needs to change the default Enge function built into COSY-∞ for quads. (It happens to be the PETRA ring quads.)

Usually, we only need to understand higher order well enough to design them to be negligible. The exceptions are the extreme conditions, for example as in a High Resolution Spectrometers and the repeated effects of higher order in storage rings. But for beam transport lines since we want them to be “sufficiently small”, approximate upper limits for the aberrations arising from individual beamline elements, are sufficient. We just calculate aberrations element by element and minimize. We don’t bother to track nonlinear effects.

Let us first determine what is meant by “sufficiently small”.

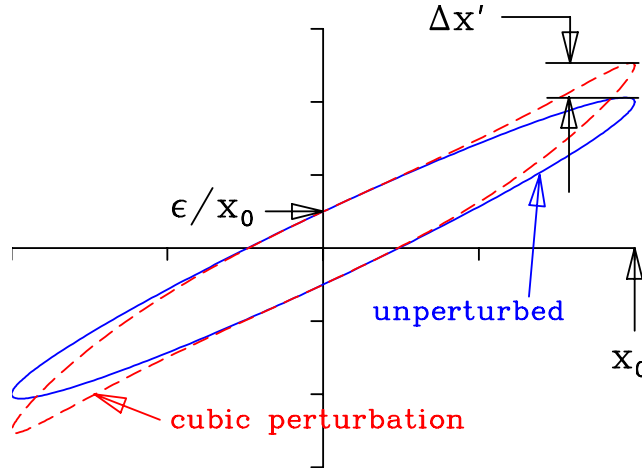


Figure 1: Phase space ellipse with cubic distortion.

The key parameter is of course the emittance. A higher order distortion is shown in Fig. 1. This may be a cubic (as is common for focusing devices where the fields are odd functions of transverse coordinates<sup>1</sup>) or parabolic in the case of the dominant error from dipoles. The order of the dominant effect is not particularly important for our purposes; only the location of the “edge” of the desired emittance matters. If desired, the expected misalignment can be included in the “size”. A high quality beam may have negligible emittance growth if it is aligned to the beamline symmetry axis, but not so when misaligned.

Let us call the integrated higher order error  $\Delta x'$ . Fig. 1 makes clear that this  $x'$  is to be compared not with the beam divergence, but with the local divergence width  $\epsilon/x_0$ , which may be significantly smaller: the two versions agree only at a waist.

The effective fractional growth in emittance is

$$\frac{\Delta\epsilon}{\epsilon} \sim \frac{\Delta x' x_0}{\epsilon}, \quad (1)$$

and we want this to be small compared to 1. How small depends upon context: typically 1% is sufficient but clearly if there are thousands of elements, we would want this to be much smaller than 1%. Most often, the emittance growth is dominated by one or two focusing elements; the ones that create the final focus.

In any beamline design, there are many constraints besides minimizing emittance growth. The main constraint is to achieve a desired match or ‘Twiss’ parameters at the final focus. This is often done by calculating the mismatch factor, which also constitutes an emittance growth. Clearly, it matters not whether growth comes from mismatch or from aberrations so these two are simply added in quadrature and the sum is minimized. This is the whole “trick” used in our code TRANSPORT. [What was wrong with the TRANSPORT approach?](#)

But it remains to find  $\Delta x'$ . This turns out to be surprisingly simple: for any of the standard beamline elements, simple formulas can be found.

## 4 Transport Elements

Solenoid third order aberration depends on aperture, or more specifically, fringe field “hardness”. Quadrupole third order aberrations do not depend

---

<sup>1</sup>Early versions of TRANSPORT extended it to only second order and so missed this effect entirely. More on this below.

on fringe field, but fifth order does. Dipole bender second order aberrations do not depend on fringe field hardness, but third order does.

## 4.1 Solenoid

Solenoids' focal strength scale as square of the ratio of magnetic field to particle momentum, while in quadrupoles, the scaling is linear, so solenoids are much weaker focusing elements than quadrupoles. For this reason, they are most commonly used for low energy electron transport. They have the great convenience that they focus both transverse directions.

It is useful to know that the magnetic field from a solenoid is completely given by the following expansions:

$$B_z(r, z) = \sum_{n=0}^{\infty} \frac{(-1)^n}{n!^2} \left(\frac{r}{2}\right)^{2n} \left(\frac{d}{dz}\right)^{2n} B_z(0, z) \quad (2)$$

$$B_r(r, z) = \sum_{n=0}^{\infty} \frac{(-1)^{n+1}}{(n+1)!n!} \left(\frac{r}{2}\right)^{2n+1} \left(\frac{d}{dz}\right)^{2n+1} B_z(0, z) \quad (3)$$

These follow directly from Maxwell's equations plus the symmetry and establishes that the fields can be completely derived in all of space, knowing only the on-axis field function.

For small  $r$ , we have:

$$B_z = B_0 - \frac{r^2}{4} B'' \quad (4)$$

$$B_r = -\frac{r}{2} B' + \frac{r^3}{16} B''' \quad (5)$$

( $B_0(z)$  is the on axis field  $B_z(0, z)$ , and  $B'$  etc. are derivatives of  $B_0(z)$ .)

To the same order,

$$B_z^2 = B_0^2 - \frac{r^2}{2} B_0 B'' \quad (6)$$

The equation of motion through the solenoid has radial part:

$$r'' + K B_z^2 r = 0 \quad (7)$$

( $K$  is a constant containing the magnetic rigidity:  $K = \frac{1}{(2B\rho)^2}$ .)

Expanding to cubic force order gives

$$r'' + K \left( B^2 r - \frac{B B''}{2} r^3 \right) = 0 \quad (8)$$

The nonlinear term gives an  $r'$  error, denoted by  $\Delta r'$ ,

$$\begin{aligned}\Delta r' &= \frac{K}{2} \int r^3 BB'' dz = \frac{K}{2} r^3 \int BB'' dz \text{ (thin lens approx.)} \\ &= -\frac{K}{2} r^3 \int B'^2 dz\end{aligned}\quad (9)$$

Thus we see that optimizing a solenoid by minimizing the off-axis focal deviation is exactly the same as minimizing the mean-squared value of  $B'$ . Solenoids' spherical aberrations diverge in the hard edge limit. This puts to rest the notion that solenoids are improved by flattening their fields, and thus shortening their fringe fields. In fact the opposite is the case: the softer the edges, the smaller the aberrations. For a long solenoid, it is beneficial to have more turns at the centre than at the entrance and exit. Again this is opposite to common practice. An example is the Rutherford Front End Test Stand[3]. If they had not flattened their solenoid fields, and had put extra turns near the centre rather than near the ends, the third order aberration would have been roughly only half as large. See also Biswas[4] on this point.

Clearly, the integral (9) depends on the form of the fringe field. However, if we can characterize it as having an effective width  $w$ , then

$$\Delta r' \sim \frac{r^3}{fwL} = \frac{r^3}{4w\rho^2}, \quad (10)$$

as the focal length for solenoids is given by  $\frac{1}{f} = \frac{\int B^2 dz}{(2B\rho)^2} = \frac{L}{4\rho^2}$ . Usually, if no special shaping is done and there is a uniform number of turns per unit length,  $w \sim 3a$  where  $a$  is aperture radius.

Roughly speaking,

$$\frac{\Delta\epsilon}{\epsilon} = \frac{\Delta r'}{\epsilon/\hat{r}} \sim \frac{\hat{r}^4}{\epsilon fwL} \quad (11)$$

## 4.2 Einzel Lens

As with solenoids, the axial symmetry of einzel or aperture lenses means that the field in all space can be determined if the on-axis field is known. In fact, the equations for electric field are identical to those for magnetic field in a solenoid eqs.2,3. Integrating the latter equation as the radial force, in the thin lens approximation, results in zero focal effect and zero aberrations. It is only when the particle's changing speed is taken into account that there is a net effect.

An einzel lens can be constructed from as few as 3 apertures; a potential plot in  $\Phi(r, z)$  is shown in Fig. 2. Near the axis, the potential is parabolic, but near

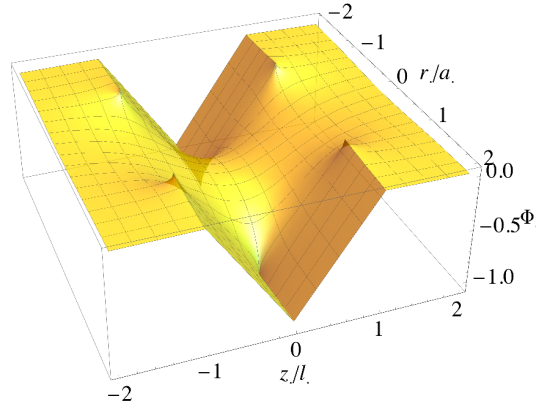


Figure 2: Potential function plot  $(r, z)$  of 3-aperture einzel lens, where apertures are at  $z = -1, 0, 1$  in units of aperture radius.

the aperture edge, it's clearly not. This can be investigated approximately by considering one aperture at a time. The grounded conducting circular aperture separating two regions that have asymptotically constant electric fields on either side is a textbook boundary value problem, for example by Jackson[5]. From this we find that in the plane of the aperture, the potential is actually elliptical, given by

$$\Phi(r, 0) = \frac{E_1}{\pi} \sqrt{a^2 - r^2} \quad (12)$$

where  $E_1$  is the electric field on the non-ground side, and  $a$  is the aperture radius. Thus, the radial electric field diverges at the aperture edge and this in itself suggests the beam should not be allowed to fill the aperture. Quadrupoles' focusing force, for example, are not singular in this way.

One can find the focal length of the single aperture by using eqn. 5 as  $E_r = -\frac{r}{2}E'$  and integrating in the thin lens limit:

$$\Delta r' = \int r'' dz = \int \frac{1}{v^2} \frac{d^2 r}{dt^2} dz = \int \frac{q}{mv^2} E_r dz \approx -\frac{r}{4V_0} E_1, \quad (13)$$

where  $qV_0 = \frac{mv^2}{2}$  and  $V_0$  is the voltage through which the beam particle of charge  $q$  has been accelerated. This a focal length  $f$ :

$$\frac{1}{f} = \frac{E_1}{4V_0}. \quad (14)$$

Clearly, this only applies in the non-relativistic regime: einzel lens are not used at relativistic energies.

Two such apertures, separated by a distance  $l$ , the first kept at the source potential  $V_0$  and the second at  $V_1 + V_0$  create the field  $E_1 = V_1/l$ . This

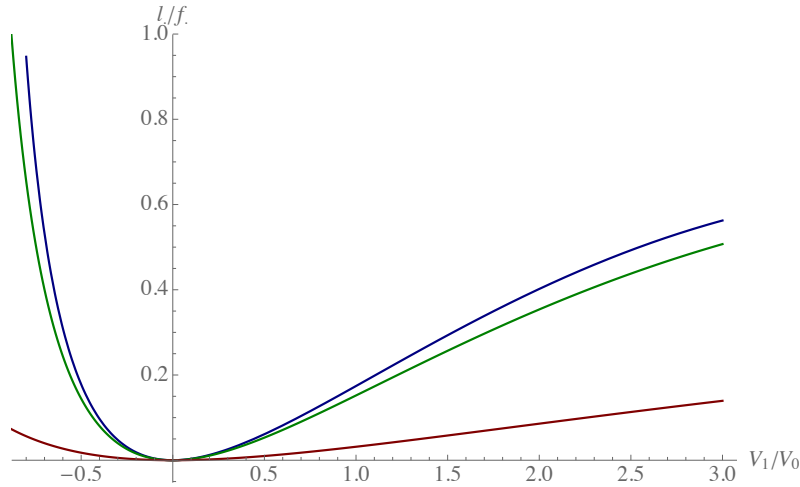


Figure 3: Focal power in units of  $1/l$  for einzel lenses. Blue: infinitesimal aperture. Green:  $a = l/10$ . Red:  $a = l$ , as drawn in Fig. 2.

constitutes an accelerator column and the focal power is known:

$$\frac{1}{f} \Big|_{\text{acc.column}} = \frac{3\kappa^2(2 + \kappa)}{8l(1 + \kappa)^2} \quad (15)$$

where  $\kappa = \sqrt{\frac{V_1 + V_0}{V_0}} - 1$  is the change in momentum relative to initial momentum. This can be derived from 3 transfer matrices: entrance aperture with  $f$  given by eq. 14 ( $f = 4V_0l/V_1$ ), body of column where  $E'_z = 0$ , and exit aperture with  $f = -4V_1l/V_0$ [6].

We create an einzel lens by placing two acceleration columns back-to-back, bringing beam energy back to source energy. The focal length of this is found to be:

$$\frac{1}{f} \Big|_{\text{einzel}} = \frac{3\kappa^2(4 - \kappa^2)}{8l(1 + \kappa)}. \quad (16)$$

The plot is the blue curve shown in Fig. 3.

Unfortunately, this expression is only accurate for cases where  $l \gg a$ , while in common practice,  $l/a \sim 4$  or less. The reason is that the superposition of apertures is not valid for small aspect ratios. This is clear from Fig. 2: The 3 apertures are not actually equipotential surfaces, and the on axis potential does not reach  $V_1 + V_0$  at lens centre.

The green and red curves of Fig. 3 were calculated using the CEA element of COSY- $\infty$ [2]. This code is an invaluable tool for calculating higher order effects in general, and in particular for realistic einzel lenses where  $a \sim l$ . COSY- $\infty$

uses the single-aperture on-axis potential as given by Jackson[5],

$$\Phi(0, z) = \frac{E_1 a}{\pi} \left[ 1 - \frac{z}{a} \cot^{-1} \left( \frac{z}{a} \right) \right], \quad (17)$$

and adds apertures together to form the lens.

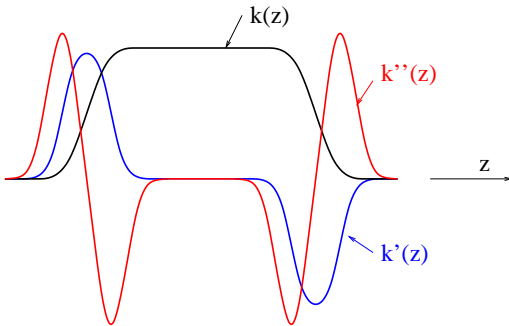
In spite of there being no closed-form expression for focal length  $f$ , we can still write the scaling for higher order effects, in terms of  $f$ . To compare with other lenses, we write in terms of the total length  $L = 2l$ . From COSY, we find

$$\Delta r' \approx \frac{r^3}{\eta f a L}, \quad (18)$$

where  $\eta$  varies according to aspect ratio: for  $L \gg a$ ,  $\eta = 3/2$ , but for example for  $L = a$ ,  $\eta = 1/2$ . Unsurprisingly, the aberrations scale similarly to solenoids as  $(faL)^{-1}$ , but for einzel lenses the proportionality factor is 2 to 6 times worse.

### 4.3 Quadrupole

Like solenoids, the lowest order aberration is cubic or third order. (BTW, please don't refer to it as 'octupole'.) But unlike solenoids, this aberration cannot be reduced by shaping the field strength function i.e. softening the edges. It turns out that the third order aberration is independent of fringe field shape or extent. (This is not however true of fifth and higher order; those in fact **are** reduced by softening the edges.[7])



The electrostatic quadrupole potential field

$$V(x, y) = \frac{k}{2}(x^2 - y^2) \quad (19)$$

is a solution to Laplace's equation, but only if the quadrupole is infinitely long ( $k=\text{constant}$ ). For finite quads, we use the expansion

$$V(x, y, z) = \frac{k}{2}(x^2 - y^2) - \frac{k''}{24}(x^4 - y^4) + \frac{k''''}{720}(x^6 - y^6) - \dots \quad (20)$$

(That's right, it does not fit the  $r^n \cos(n\theta)$  multipolar expansion.) The quartic term gives a cubic force term which leads to the following focusing error,

$$\Delta x' = \frac{-1}{f^2 L_Q} \left( \frac{7}{6} x^3 - \frac{1}{2} x y^2 \right), \quad (21)$$

where  $L_Q$  is the quad length and  $f$  the focal length. It is important to note that this is independent of aperture size or fringe field hardness: indeed, the aberration is not affected by changing the fringe field shape.

For the Hamiltonian technique used to derive these, see article[8]. I further refine electrostatic for the relativistic case[9]:

$$\Delta x' = \frac{-1}{f^2 L_Q} \left( \frac{7 - 3\beta^2}{6} x^3 - \frac{1 - \beta^2}{2} x y^2 \right). \quad (22)$$

The formula for magnetic quads is similar:

$$\Delta x' = \frac{-1}{f^2 L_Q} \left( \frac{1}{3} x^3 + x y^2 \right), \quad (23)$$

So electrostatic quads are not really worse than magnetic quads; might actually be better for e.g. ribbon beams.

For both cases, let's say  $\Delta x' = \frac{-1}{f^2 L_Q} (Ax^3 + Bxy^2)$ , where  $A \sim B \sim 1$ . Roughly speaking,

$$\frac{\Delta \epsilon}{\epsilon} = \frac{\Delta x'}{\epsilon / \hat{x}} \sim \frac{\hat{x}^4}{\epsilon f^2 L_Q} \quad (24)$$

This formula has an obvious consequence: In any transport system where **optics strengths and beam sizes are given**, the only way to reduce emittance growth due to aberrations is to **lengthen** the “worst-offending” quadrupoles. Further, damaging effects scale as beam size to the **fourth** power. This can mean that some quads may have to be **shortened**.

To reiterate, (1) ‘large’ does **not** mean large aperture occupation fraction, (2) fiddling with fringe-field-shape gains nothing in 3rd order. (Off topic: it does gain in 5th and higher, where softer fringe fields result in lower aberration; opposite to intuition!)

#### 4.3.1 Quad Match Example

We apply this to the example shown in the Fig. 4. The RFQ requires matched  $\beta_T = 6.125$  cm and the beam comes from a FODO section where  $\beta_T = 84.6$  cm.

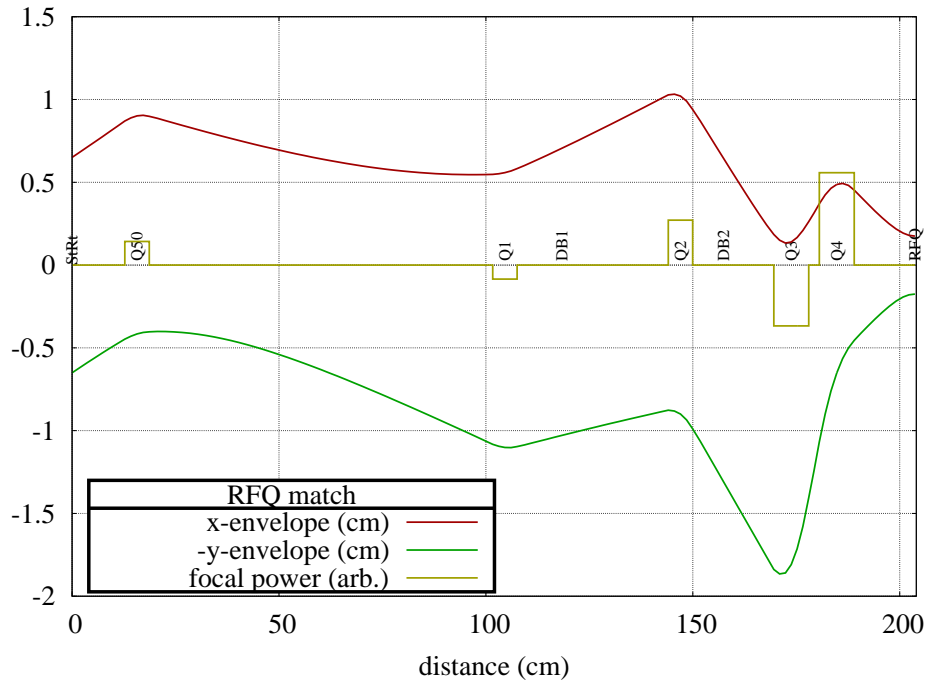


Figure 4: First order beam envelopes for match to RFQ. Emittance is  $50 \mu\text{m}$ . Red is  $x$ -envelope, green is  $y$ -envelope, plotted for clarity as if it is negative. Yellow is the quadrupole strength function. This is for exact first order match ignoring the third order aberrations. Emittance growth is very bad as can be seen in blue curve of Fig. 6

With final quadrupoles of effective length  $L = 8.4 \text{ cm}$ , we get  $\hat{x} = 1.8 \text{ cm}$ ,  $f = 9.7 \text{ cm}$ , with desired acceptance  $\epsilon = 0.005 \text{ cm}^2$ . We get

$$\frac{\Delta\epsilon}{\epsilon} \sim \frac{1.8^4}{0.005 \times 9.7^2 \times 8.4} = 2.6 \quad (25)$$

To improve the emittance growth, we shorten the final quad in order to decrease the size of the beam in the next-to-final quad. In this case (Fig. 5), beam size is only one half as large, so result is 1/16 or

$$\frac{\Delta\epsilon}{\epsilon} \sim 0.17. \quad (26)$$

These calculations were verified with COSY- $\infty$ [2] and gave  $\frac{\Delta\epsilon}{\epsilon} \approx 0.1$ . Final phase spaces are shown in Fig. 6.

It is important to understand that codes like TRANSPORT and TRACE3D can result in aberrations as large as that of the blue curve in Fig. 6, without any hint that there is a problem.

Input files for this case are as follows: Transport subroutine:

<sup>2</sup>commonly: “ $50\pi \text{ mm-mrad}$ ”

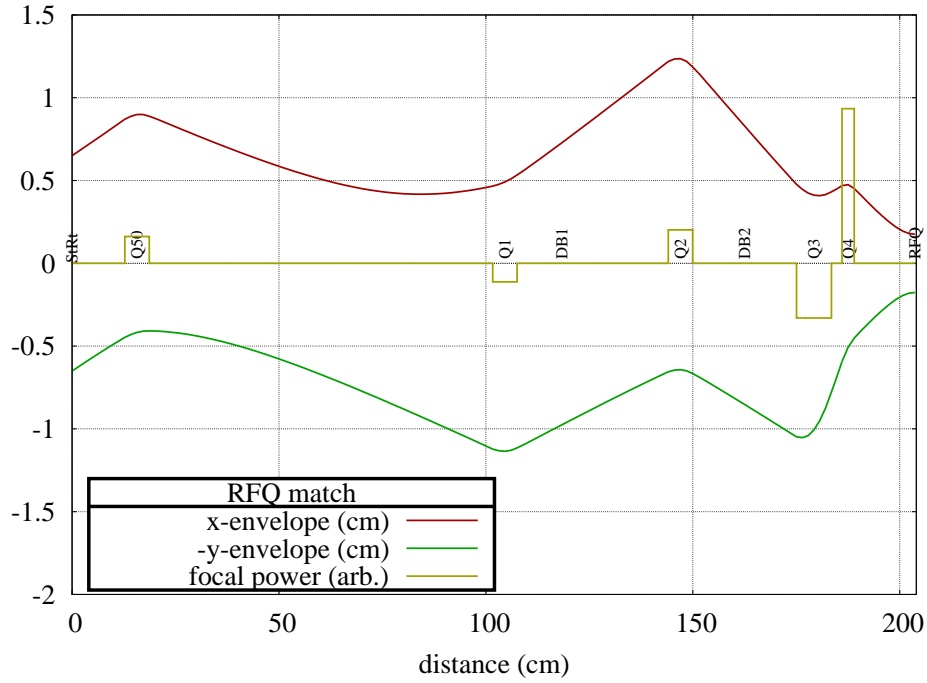


Figure 5: Optimized RFQ match, taking into account third order aberrations according to equation 21.

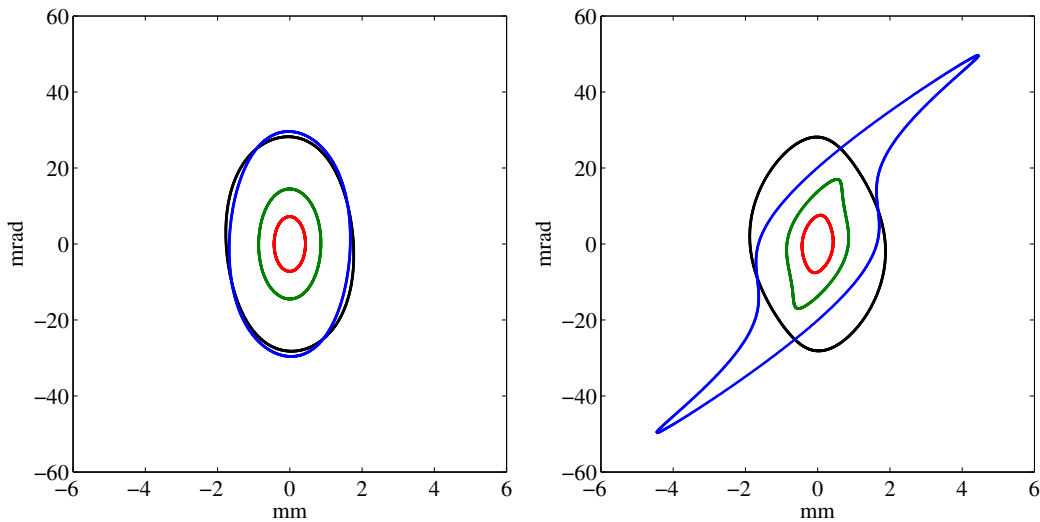


Figure 6: These calculations were verified with COSY- $\infty$ . Emittance contours (i.e. constant action) in phase space for previous envelope figures. Left is  $x-P_x$ , right is  $y-P_y$ . These were calculated from the COSY- $\infty$  transfer maps. Black is the optimized case for the design acceptance  $\epsilon = 50 \mu\text{m}$ , where the long next-to-last quad is brought forward by shrinking the final quad, as shown in Fig. 5. Blue, green and red are for the non-optimum configuration: blue is the matched beam  $\epsilon = 50 \mu\text{m}$ , green is for  $\epsilon = 12.5 \mu\text{m}$ , red is for  $\epsilon = 3 \mu\text{m}$ .

```

SUBROUTINE SYSTEM
COMMON /BLOC1/q0,q1,q2,q3,q4,d2,d3,d4,d5,xcm,ycm,wab
d1=63.7205-d2-d3-d4-d5
call DRIFT(                    5.0205,'.  ')
call EQUAD(  q0      ,  2.5400,  2.3200,wab,'Q-periodic')
call DRIFT(                    d1,'.  ')
call EQUAD( -q1      ,  2.5400,  2.3200,wab,'IRA:Q1')
call DRIFT(                    d2,'.  ')
call EQUAD(  q2      ,  2.5400,  2.3200,wab,'IRA:Q2')
call DRIFT(                    d3,'.  ')
call EQUAD( -q3      ,  2.5400,  3.3200,wab,'IRA:Q3')
call DRIFT(                    d4,'.  ')
call EQUAD(  q4      ,  1.2700,  1.1600,wab,'IRA:Q4')
call DRIFT(                    d5,'waist')
call match(1,xcm,1.,1) !1 means x weight = 1.
call match(3,ycm,1.,1) !3 means y
RETURN
END

```

Data file:

```

0.060 0 0 27930.0 1 0. !60keV, mass=30u
1 3 5. 0.5E-5
0 -0.
0.65054 18.4506 .65054 18.4506 1.5 0.476 !initial beam
1. 1000. 1. 1000. 1. 100. 0. .3937008 !units
3 !correlation parameters
1 2 0.909106
3 4 -0.909106
5 6 -1.
12 !number of parameters
0.000 .0 5.0 1 !5 quad strengths
0.000 .0 5.0 1
0.000 .0 5.0 1
0.000 .0 5.0 1
0.000 .0 5.0 1
8.0000 0. 60. 1 !inter-quad spacings
8.00 0. 60. 1
8.00 0. 60. 1
8.00 0. 60. 1
0.175 0. 1. 0 !waist size
0.175 0. 1. 0
5. 0. 100. 0 !weight for quad aberration deps/eps
1.E-6 900

```

03 1. 0.98 50

## 4.4 Dipole Bender

Dipole magnets or electrostatic benders are similar to quadrupoles in that their lowest order aberrations are insensitive to field falloff shaping and extent. The difference is that the lowest order is quadratic rather than cubic force. See my Snowmass talk[10] for derivations.

For the sector magnet, the nonlinear kicks are as follows ( $L = \rho\theta$ , the trajectory length):

$$\Delta x' = -\frac{L}{2\rho^3}y^2 \text{ and } \Delta y' = -\frac{L}{\rho^3}xy \quad (27)$$

Often for dipoles, the length  $L$  is not small compared with the focal length, so the thin lens approximation used in estimating the aberration is not very good. In that case, the calculation can simply split the dipole once or twice.

For the electrostatic dipole bender, I've solved the general toroidal case. Here,  $c$  is the ratio of electrode curvature in the bend plane to the non-bend plane. This means  $c = 0$  is a cylindrical bend and  $c = 1$  is a spherical one.

$$\Delta x' = \frac{L}{\rho^3} \left[ \left( -4 + \frac{7}{2}c - c^2 \right) x^2 + \left( -\frac{1}{2}c + c^2 \right) y^2 \right] \quad (28)$$

$$\Delta y' = \frac{L}{\rho^3} (-c + 2c^2) xy \quad (29)$$

## 5 Summary of Higher Order Kick Formulas

Table 1: Higher order kicks for a few chosen common elements.

Element	$\Delta x'$	$\Delta y'$
<b>Solenoid</b> <i>w</i> =fringe field length, <i>f</i> =focal length, <i>L</i> =eff. length	$-\frac{x(x^2+y^2)}{fwL}$	$-\frac{y(x^2+y^2)}{fwL}$
<b>Einzel Lens</b> <i>a</i> =aperture radius, <i>f</i> =focal length, <i>L</i> =total length, $1/2 < \eta < 3/2$	$-\frac{x(x^2+y^2)}{\eta faL}$	$-\frac{y(x^2+y^2)}{\eta faL}$
<b>Magnetic Quadrupole</b> <i>f</i> =focal length, <i>L</i> =eff. length	$\frac{-1}{f^2L} \left( \frac{1}{3}x^3 + xy^2 \right)$	$\frac{-1}{f^2L} \left( \frac{1}{3}y^3 + yx^2 \right)$
<b>Electric Quadrupole</b>	$\frac{-1}{f^2L} \left( \frac{7}{6}x^3 - \frac{1}{2}xy^2 \right)$	$\frac{-1}{f^2L} \left( \frac{7}{6}y^3 - \frac{1}{2}yx^2 \right)$
<b>Magnetic Sector Bend</b> $\theta$ =bend angle, $\rho$ =bend radius	$-\frac{\theta y^2}{2\rho^2}$	$-\frac{\theta xy}{\rho^2}$
<b>Electric Cylindrical Bend</b>	$-\frac{4\theta x^2}{\rho^2}$	0
<b>Electric Spherical Bend</b>	$\frac{\theta(-3x^2+y^2)}{2\rho^2}$	$\frac{\theta xy}{\rho^2}$

## 6 Growth from mismatch

The mismatch factor is the standard definition from e.g. Bovet et al.[11]. See Fig. 7. The ratio of area of the ellipse that is similar but encapsulates the mismatched ellipse, to the area of the mismatched ellipse, is  $D + \sqrt{D^2 - 1}$  where  $D \equiv (\beta_2\gamma_1 + \beta_1\gamma_2)/2 - \alpha_1\alpha_2$  and  $\alpha, \beta, \gamma$  are the ‘Twiss’ parameters of the mismatched ellipse (subscript 1) and the matched ellipse (subscript 2). As  $D - 1 \ll 1$ , it is sufficient to summarize this as  $\Delta\epsilon/\epsilon \approx \sqrt{2(D - 1)}$ .

$$\begin{aligned} \text{where } D &= \frac{1}{2} (\beta_2\gamma_1 + \gamma_2\beta_1 - 2\alpha_1\alpha_2) \\ &= 1 + \frac{(L_2 - L_1)^2 + (S_2 - S_1)^2}{2L_1L_2} . \end{aligned}$$

For meaning of  $\alpha, \beta, \gamma, L, S$  see 3.2 .

### 3.4.5 Three ellipses

- a) Area of ellipse  $S_3$ , similar to  $S_2$ , such that  $S_3$  circumscribes  $S_1$ : (area  $S_1 = \text{area } S_2 = S$ )

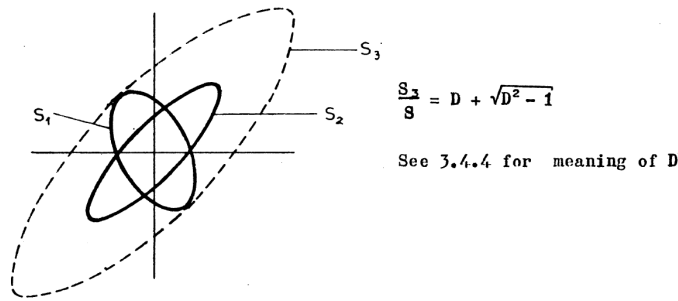


Figure 7: Excerpt from Bovet et al.[11]

## 7 TRANSOPTR: Beam Transport Optimization technique

Emittance growth factors are found for each transport element and combined with the emittance growth due to mismatch, to form a function to be minimized. We simply add (in quadrature) together, and minimize this as we vary parameters such as quad position, length, strengths.

This does not pretend to be a higher order calculation; indeed, it is possible (though highly unlikely) that the higher order of one element is compensated by another, and this would only show up in an actual higher order calculation.

As stated, the intention is not to find accurate higher order effects, only to ensure that they are negligible.

## 7.1 Optimization Engine

There are many optimization techniques for designing and tuning beam transport lines. Some are built into the transport codes themselves. Almost all of these work on the basis of reducing an error to zero by finding local derivatives of the error with respect to the parameters. I use a downhill simplex method. It's fast and robust.

It is also easily modified to incorporate simulated annealing for more than 3 free parameters. I use routines from the book *Numerical Recipes* by Press, Flannery, et al.[12]

Applied to the design of a transport channel we proceed as follows.

1. Choose a set of parameters such as quad strengths, locations, and their allowed ranges.
2. The “temperature” is the fraction of the full range of variation of any parameter, so at  $T = 1$ , all parameters vary randomly through their full ranges.
3. The sum ( $\chi$ ) of all possible effects to be minimized, such as mismatch, emittance growth, etc. with their appropriate weights, is calculated for each of  $N$  parameter sets.
4. A region in parameter space is chosen that contains the best values, but the volume of the region is shrunk by reducing  $T$ , multiplying it by a factor  $\alpha (< 1)$ .
5. This continues until either  $T$  or  $\chi$  is smaller than some tolerance (typically  $10^{-4}$  for single precision).

For as few as 3 parameters,  $\alpha$  can be 0.88, with  $N = 8$ , resulting in only about 100 evaluations of the beamline to achieve  $10^{-4}$  accuracy. But this number of evaluations increases exponentially with number of parameters.

As example, we take the RFQ match mentioned above. See animation (or try this one).

Input files for this case are as follows: Transport subroutine:

```
SUBROUTINE tSYSTEM
```

```
COMMON /BLOC1/q0,q1,q2,q3,q4,d2,d3,d4,d5,xcm,ycm,wab
d1=63.7205-d2-d3-d4-d5
call DRIFT(          5.0205,'.  ')
call EQUAD(  q0    ,  2.5400,  2.3200,wab,'Q-periodic')
call DRIFT(          d1,'.  ')
call EQUAD( -q1    ,  2.5400,  2.3200,wab,'IRA:Q1')
call DRIFT(          d2,'.  ')
call EQUAD(  q2    ,  2.5400,  2.3200,wab,'IRA:Q2')
call DRIFT(          d3,'.  ')
call EQUAD( -q3    ,  2.5400,  3.3200,wab,'IRA:Q3')
call DRIFT(          d4,'.  ')
call EQUAD(  q4    ,  1.2700,  1.1600,wab,'IRA:Q4')
call DRIFT(          d5,'waist')
call match(1,xcm,1.,1) !1 means x weight = 1.
call match(3,ycm,1.,1) !3 means y
RETURN
END
```

Data file:

```

0.060 0 0 27930.0 1 0. !60keV, mass=30u
1 3 5. 0.5E-5
0 -0.
0.65054 18.4506 .65054 18.4506 1.5 0.476 !initial beam
1. 1000. 1. 1000. 1. 100. 0. .3937008 !units
3 !correlation parameters
1 2 0.909106
3 4 -0.909106
5 6 -1.
12 !number of parameters
    0.000 .0 5.0 1 !5 quad strengths
    0.000 .0 5.0 1
    0.000 .0 5.0 1
    0.000 .0 5.0 1
    0.000 .0 5.0 1
8.0000 0. 60. 1 !inter-quad spacings
8.00 0. 60. 1
8.00 0. 60. 1
8.00 0. 60. 1
    0.175 0. 1. 0 !waist size
    0.175 0. 1. 0
    5. 0. 100. 0 !weight for quad aberration deps/eps
1.E-6 900
03 1. 0.98 50

```

8 free parameters required 140,000 calls to the transport system subroutine, 7.4 seconds CPU time (M3 Mac). Others:

free parameters	Calls	CPU on Mac
8	140,000	7.4 s
7	13,000	0.71 s
6	1,700	0.11 s
5	825	0.06 s
4	215	0.03 s

N.B.: In this example, almost any arrangement with 4 parameters (typically, just the 4 quad strengths) can yield an exact match to the RFQ. But there is only one best arrangement of quad spacing that minimizes aberrations. That requires all 8 parameters.

Just for fun, here is a larger example but run from a GUI:

Matching demo. First let Q5,7,8 vary to get better match. Fix them, set final 4 quads to vary and adjust Q50. Watch how it maintains the match to the RFQ.

## 8 Conclusions – non-integration cases

Simple formulas for the lowest order aberrations and can be used to estimate emittance growth. A simple strategy for beam transport system design optimization is to add these growths to the growth from mismatch, to form an error function to be minimized. Efficient first order transport codes (with or without space charge) can be augmented in this way. An example is TRANSOPTR, which uses a minimization engine to vary beamline parameters to find an optimum with negligible emittance growth.

At TRIUMF, many beamlines have been efficiently designed in this way, and perform as predicted.

## 9 TRANSOPTR: Integration mode

TRANSOPTR[16] was originally written in 1981. It, like the original envelope codes TRANSPORT and TRACE3D included only elements whose transfer matrices could be written in closed form and were known. As stated above, this required all elements to be “hard-edged”: to get anything more accurate would require chopping into bits.

Similarly, the first attempts to extend to include space charge were a real kludge: to subdivide elements and interleave defocus thin lenses to carry the linear part of the space charge force. (Some codes in use - TRACE3D, I believe - still do this.) The right way to do it is to derive the equations of motion of the  $\sigma$  matrix elements and have envelope code itself numerically integrate through the elements. The exact differential equations of Sacherer[17] were incorporated into TRANSOPTR by **Mark deJong**[18], for the express purpose of including space charge.

History: Already in 1959[19], Kapchinsky and Vladimirov had found the equations of envelope evolution for case of continuous beams uniform in configuration and phase space. Seems too highly idealized to be useful, right? Also severely limited as cannot include any coupling, either between transverse directions or with longitudinal. I’ll show how theirs was a special case for a very general formalism.

In 1970, Frank Sacherer[17] showed that the same equations result from finding the equations of motion of the beam envelope (the second moments of the beam distribution). But his more general formalism allowed for any linear forces, including coupling, dispersion, etc. and further extended it to bunched beams.

## 9.1 Statistical Approach to Beam Dynamics

If there is a distribution of particles, one would like to calculate the final distribution from the initial. The behaviour of the beam centroid

$$\langle \mathbf{X} \rangle = \sum_{i=1}^N \mathbf{X}_i / N \quad (30)$$

(where  $N$  is the number of particles, and  $\mathbf{X}$  is the column vector  $(x, P_x, y, P_y, z, P_z)^T$  as in eqn. 36) is determined by the same transfer matrix  $\mathbf{M}$  as for an individual particle. This is the equation of ‘first moments’. At the next level, one would like to calculate the evolution of the beam widths, or, ‘second moments’ given by

$$\boldsymbol{\sigma} \equiv \frac{1}{N} \sum_{i=1}^N \mathbf{X}_i \mathbf{X}_i^T \quad (31)$$

For example,  $\sigma_{11} = \langle x^2 \rangle$ ,  $\sigma_{12} = \langle xP_x \rangle$ ,  $\sigma_{13} = \langle xy \rangle$ , .... For a distribution of particles so dense that we do not see graininess on any scale of our diagnostics, the sums go over into integrals. For example,

$$\sigma_{12} = \int \int \int \int \int \int x P_x f(x, P_x, y, P_y, z, P_z) dx dP_x dy dP_y dz dP_z,$$

where  $f$  is the distribution in phase space, normalized so that its integral over all 6 phase space dimensions is 1.

Here,  $s$  is the independent variable, and as will be shown, the longitudinal coordinates are:  $z = \beta c \Delta t$ ,  $P_z = (\beta c)^{-1} \Delta E$ .

By direct substitution into the definition of  $\boldsymbol{\sigma}$ , we find

$$\boldsymbol{\sigma}_f = \mathbf{M} \boldsymbol{\sigma}_i \mathbf{M}^T \quad (32)$$

The transfer matrix  $\mathbf{M} = \mathbf{I} + \mathbf{F} ds$  over an infinitesimal length  $ds$  gives the equations of motion of individual particles:

$$\mathbf{X}' = \mathbf{F} \mathbf{X}. \quad (33)$$

We find directly the differential equation for  $\boldsymbol{\sigma}$ :

$$\boldsymbol{\sigma}' = \mathbf{F} \boldsymbol{\sigma} + \boldsymbol{\sigma} \mathbf{F}^T. \quad (34)$$

This is the **envelope equation**. For the full 6D case, it represents 21 equations. (Because  $\boldsymbol{\sigma}$  is symmetric.)

## 9.2 What is F? Infinitesimal Transfer Matrix

The general Hamiltonian can be Taylor-expanded by orders in the 6 dependent variables<sup>3</sup>,

$$H(x_1, x_2, x_3, x_4, x_5, x_6; s) = \sum_i \frac{\partial H}{\partial x_i} \Big|_0 x_i + \frac{1}{2} \sum_{i,j} \frac{\partial^2 H}{\partial x_i \partial x_j} \Big|_0 x_i x_j + \dots \quad (35)$$

The subscript 0 means that the derivatives are evaluated on the reference trajectory  $\forall i, x_i = 0$ . (Keep in mind though that these partial derivatives in general are functions of the independent variable  $t$  or  $s$ .)

Terms of first order are eliminated by transforming to a coordinate system measured with respect to the reference trajectory (the Frenet-Serret system). The remaining terms are second order and higher, and for linear motion, we simply truncate at the second order.

Then the Hamiltonian looks like  $H = Ax^2 + BxP_x + Cxy + \dots + UP_z^2$ : there are 21 independent terms.  $A = \frac{1}{2} \frac{\partial^2 H}{\partial x^2}$ , and so on; all derivatives are evaluated on the reference trajectory, and may be a function of the independent variable. We know the equations of motion from the Hamiltonian to be:  $x' = \partial H / \partial P_x$ ,  $P_x' = -\partial H / \partial x$ , etc., where primes denote derivatives w.r.t. the independent variable. Therefore the equations of motion:

$$\begin{pmatrix} x' \\ P_x' \\ y' \\ P_y' \\ z' \\ P_z' \end{pmatrix} = \begin{pmatrix} \frac{\partial^2 H}{\partial P_x \partial x} & \frac{\partial^2 H}{\partial P_x^2} & \frac{\partial^2 H}{\partial P_x \partial y} & \frac{\partial^2 H}{\partial P_x \partial P_y} & \frac{\partial^2 H}{\partial P_x \partial z} & \frac{\partial^2 H}{\partial P_x \partial P_z} \\ -\frac{\partial^2 H}{\partial x^2} & -\frac{\partial^2 H}{\partial x \partial P_x} & -\frac{\partial^2 H}{\partial x \partial y} & -\frac{\partial^2 H}{\partial x \partial P_y} & -\frac{\partial^2 H}{\partial x \partial z} & -\frac{\partial^2 H}{\partial x \partial P_z} \\ \frac{\partial^2 H}{\partial P_y \partial x} & \frac{\partial^2 H}{\partial P_y \partial P_x} & \frac{\partial^2 H}{\partial P_y \partial y} & \frac{\partial^2 H}{\partial P_y^2} & \frac{\partial^2 H}{\partial P_y \partial z} & \frac{\partial^2 H}{\partial P_y \partial P_z} \\ -\frac{\partial^2 H}{\partial y \partial x} & -\frac{\partial^2 H}{\partial y \partial P_x} & -\frac{\partial^2 H}{\partial y^2} & -\frac{\partial^2 H}{\partial y \partial P_y} & -\frac{\partial^2 H}{\partial y \partial z} & -\frac{\partial^2 H}{\partial y \partial P_z} \\ \frac{\partial^2 H}{\partial P_z \partial x} & \frac{\partial^2 H}{\partial P_z \partial P_x} & \frac{\partial^2 H}{\partial P_z \partial y} & \frac{\partial^2 H}{\partial P_z \partial P_y} & \frac{\partial^2 H}{\partial P_z^2} & \frac{\partial^2 H}{\partial P_z \partial P_z} \\ -\frac{\partial^2 H}{\partial z \partial x} & -\frac{\partial^2 H}{\partial z \partial P_x} & -\frac{\partial^2 H}{\partial z \partial y} & -\frac{\partial^2 H}{\partial z \partial P_y} & -\frac{\partial^2 H}{\partial z^2} & -\frac{\partial^2 H}{\partial z \partial P_z} \end{pmatrix} \begin{pmatrix} x \\ P_x \\ y \\ P_y \\ z \\ P_z \end{pmatrix} \quad (36)$$

or,

$$\mathbf{X}' = \mathbf{F}\mathbf{X}, \quad (37)$$

where  $\mathbf{F}$  is called the ‘infinitesimal transfer matrix’. Or in other words, if we define  $\mathbf{H} := \frac{\partial^2 H}{\partial x_i \partial x_j}$ , i.e. the Hessian, and  $\mathbf{S}$  as the fundamental symplectic matrix

$$\mathbf{S} = \begin{pmatrix} 0 & 1 & 0 & 0 & 0 & 0 \\ -1 & 0 & 0 & 0 & 0 & 0 \\ 0 & 0 & 0 & 1 & 0 & 0 \\ 0 & 0 & -1 & 0 & 0 & 0 \\ 0 & 0 & 0 & 0 & 0 & 1 \\ 0 & 0 & 0 & 0 & -1 & 0 \end{pmatrix},$$

<sup>3</sup>In this shorthand,  $x_1 = x, x_2 = P_x, x_3 = y, \dots$

then

$$\mathbf{F} = \mathbf{SH}.$$

Of the 36 elements of  $\mathbf{F}$  there are only 21 independent ones. Easily integrated if  $\mathbf{F}=\text{constant}$ , directly as

$$\mathbf{X}_{\text{final}} = \mathbf{M}\mathbf{X}_{\text{initial}}$$

where

$$\mathbf{M} = \exp[\mathbf{F}s] = \mathbf{I} + \mathbf{F}s + \frac{1}{2}\mathbf{F}^2s^2 + \frac{1}{3!}\mathbf{F}^3s^3 + \dots,$$

Try this with the quadrupole case:

$$\mathbf{F} = \begin{pmatrix} 0 & 1 \\ -k & 0 \end{pmatrix}.$$

You just need the powers of  $\mathbf{F}$ , which are very easy in this case. Out will pop the Taylor series of the sines and cosines.

This is an approach that goes back to the 50's and MURA. Here is Don Edwards and Lee Teng from 1973 [20]:

© 1973 IEEE. Personal use of this material is permitted. However, permission to reprint/republish this material for advertising or promotional purposes or for creating new collective works for resale or redistribution to servers or lists, or to reuse any copyrighted component of this work in other works must be obtained from the IEEE.

**PARAMETRIZATION OF LINEAR COUPLED MOTION  
IN PERIODIC SYSTEMS**

D. A. Edwards and L. C. Teng  
National Accelerator Laboratory\*  
Batavia, Illinois

...

$$\mathbf{S} = \begin{pmatrix} 0 & 1 \\ -1 & 0 \end{pmatrix} \quad \mathbf{S} = \begin{pmatrix} 0 & 1 & 0 & 0 \\ -1 & 0 & 0 & 0 \\ 0 & 0 & 0 & 1 \\ 0 & 0 & -1 & 0 \end{pmatrix} \quad (1)$$

A "prime" will imply differentiation with respect to the independent variable  $z$ . The transpose of a matrix  $A$  is  $A^T$ , the trace is  $\text{Tr}A$ , and the determinant is  $|A|$ .

Statement of the Problem

We consider a two-dimensional system described by the Hamiltonian

$$H = \frac{1}{2}(p_x^2 + p_y^2) + L(p_x y - p_y x) + \frac{1}{2}F x^2 + Kxy + \frac{1}{2}G y^2 \quad (2)$$

where  $x$  and  $y$  are orthogonal coordinates,  $p_x$  and  $p_y$  are their conjugate momenta, and  $L, F, K,$  and  $G$  are periodic in  $z$  with a period of  $C$ . This form of the Hamiltonian may describe coupled betatron oscillations in a synchrotron, in which case  $K$  and  $L$  would arise from skew quadrupole and solenoidal fields, respectively. However, any bilinear Hamiltonian can be brought to this form by a suitable canonical transformation.

In matrix notation, (2) is

$$H = \frac{1}{2}\mathbf{X}^T \mathbf{H} \mathbf{X}$$

with

$$\mathbf{X} \equiv \begin{pmatrix} x \\ p_x \\ y \\ p_y \end{pmatrix}; \quad \mathbf{H} \equiv \begin{pmatrix} F & 0 & K & -L \\ 0 & 1 & L & 0 \\ K & L & G & 0 \\ -L & 0 & 0 & 1 \end{pmatrix}$$

The canonical equations may be written

$$\mathbf{X}' = \mathbf{Q}\mathbf{X}$$

where

$$\mathbf{Q} = \mathbf{S}\mathbf{H} = \begin{pmatrix} 0 & 1 & L & 0 \\ -F & 0 & K & L \\ -L & 0 & G & 1 \\ -K & -L & -G & 0 \end{pmatrix}$$

and  $\mathbf{S}$  is the matrix defined in (1).

A particular case is where the beamline consists only of elements that keep all 3 degrees of freedom independent of each other, and there is only focusing

forces  $F(s)$  and  $-G(s)$  that vary with  $s$ . In other words, the Hamiltonian is 38,

$$H = \frac{P_x^2}{2} + F(s) \frac{x^2}{2} + \frac{P_y^2}{2} + G(s) \frac{y^2}{2} + \frac{P_z^2}{2\gamma^2} \quad (38)$$

so

$$\mathbf{F} = \begin{pmatrix} 0 & 1 & 0 & 0 & 0 & 0 \\ -F & 0 & 0 & 0 & 0 & 0 \\ 0 & 0 & 0 & 1 & 0 & 0 \\ 0 & 0 & -G & 0 & 0 & 0 \\ 0 & 0 & 0 & 0 & 0 & \frac{1}{\gamma^2} \\ 0 & 0 & 0 & 0 & 0 & 0 \end{pmatrix} \quad (39)$$

(These give the standard Hill equations  $x'' + F(s)x = 0$ ,  $y'' + G(s)y = 0$ , and also  $z' = P_z/\gamma^2 = \text{constant}$ .)

### 9.3 Example: Quadrupole (Hard-edge)

Then force coefficients are constant:  $F(s) = K^2$ ,  $G(s) = -K^2$  (i.e. constants; not functions of  $s$ ), in Mathematica using MatrixExp:

$$\begin{aligned} & \text{MatrixExp} \left[ \left( \begin{pmatrix} 0 & 1 & 0 & 0 \\ -K^2 & 0 & 0 & 0 \\ 0 & 0 & 0 & 1 \\ 0 & 0 & K^2 & 0 \end{pmatrix} L \right) \right] = \\ & = \begin{pmatrix} \text{Cos}[KL] & \frac{\text{Sin}[KL]}{K} & 0 & 0 \\ -K\text{Sin}[KL] & \text{Cos}[KL] & 0 & 0 \\ 0 & 0 & \text{Cosh}[KL] & \frac{\text{Sinh}[KL]}{K} \\ 0 & 0 & K\text{Sinh}[KL] & \text{Cosh}[KL] \end{pmatrix} \end{aligned}$$

### 9.4 Example: Solenoid (Hard-edge)

$K(s) = \frac{B(s)}{2B\rho}$  is often as in TRANSPORT approximated as constant (hard-edge). **Not** a good approximation for short solenoids as in electron injectors.

If constant,

$$\text{MatrixExp} \left[ \left( \begin{pmatrix} 0 & 1 & K & 0 \\ -K^2 & 0 & 0 & K \\ -K & 0 & 0 & 1 \\ 0 & -K & -K^2 & 0 \end{pmatrix} L \right) \right] =$$

$$= \begin{pmatrix} \text{Cos}[KL]^2 & \frac{\text{Sin}[2KL]}{2K} & \text{Cos}[KL]\text{Sin}[KL] & \frac{\text{Sin}[KL]^2}{K} \\ -\frac{1}{2}K\text{Sin}[2KL] & \text{Cos}[KL]^2 & -K\text{Sin}[KL]^2 & \text{Cos}[KL]\text{Sin}[KL] \\ -\frac{1}{2}\text{Sin}[2KL] & -\frac{\text{Sin}[KL]^2}{K} & \text{Cos}[KL]^2 & \frac{\text{Sin}[2KL]}{2K} \\ K\text{Sin}[KL]^2 & -\frac{1}{2}\text{Sin}[2KL] & -\frac{1}{2}K\text{Sin}[2KL] & \text{Cos}[KL]^2 \end{pmatrix}$$

$$\text{Apply Rotation: } \mathbf{Rot}[A.] = \begin{pmatrix} \text{Cos}[A] & 0 & \text{Sin}[A] & 0 \\ 0 & \text{Cos}[A] & 0 & \text{Sin}[A] \\ -\text{Sin}[A] & 0 & \text{Cos}[A] & 0 \\ 0 & -\text{Sin}[A] & 0 & \text{Cos}[A] \end{pmatrix};$$

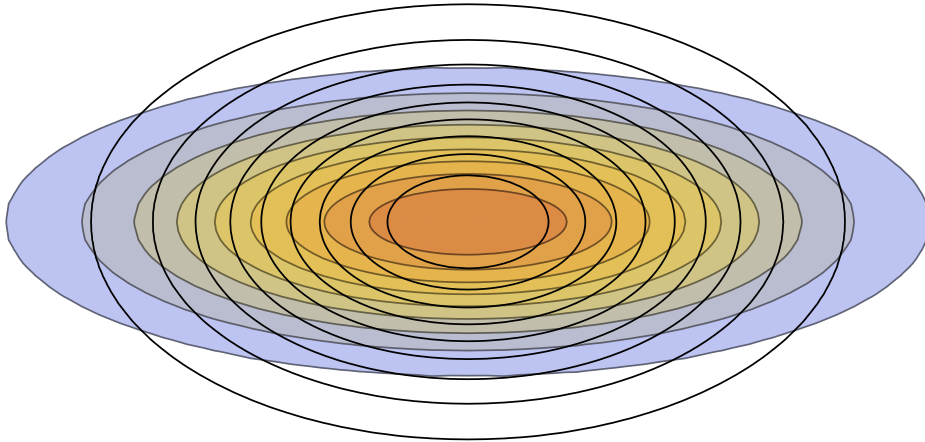
$$\mathbf{Rot}[-KL].\mathbf{M}] = \begin{pmatrix} \text{Cos}[KL] & \frac{\text{Sin}[KL]}{K} & 0 & 0 \\ -K\text{Sin}[KL] & \text{Cos}[KL] & 0 & 0 \\ 0 & 0 & \text{Cos}[KL] & \frac{\text{Sin}[KL]}{K} \\ 0 & 0 & -K\text{Sin}[KL] & \text{Cos}[KL] \end{pmatrix}$$

## 9.5 Space Charge part of F

But space charge is somewhat different.

### 9.5.1 Space Charge with Uniform elliptical beam

While for both a round beam and a flat beam, the equipotentials have the same shape as the charge density contours, the in-between case does **not**.



Density

contours aspect ratio  $\frac{a}{b}$ , but equipotential contours  $\sqrt{\frac{a}{b}}$ .

For a uniformly populated elliptical beam, semi-axis  $a$  in the  $x$ -direction and

$b$  in the  $y$ -direction, the electric field inside the beam becomes

$$\begin{aligned}\mathcal{E}_x &= \frac{\lambda}{2\pi\epsilon_0} \frac{2x}{a(a+b)} = \frac{\lambda}{4\pi\epsilon_0} \frac{x}{\tilde{x}(\tilde{x} + \tilde{y})} = \frac{I \times 30 \Omega}{\beta} \frac{x}{\tilde{x}(\tilde{x} + \tilde{y})} \\ \mathcal{E}_y &= \frac{\lambda}{2\pi\epsilon_0} \frac{2y}{b(a+b)} = \frac{\lambda}{4\pi\epsilon_0} \frac{y}{\tilde{y}(\tilde{x} + \tilde{y})} = \frac{I \times 30 \Omega}{\beta} \frac{y}{\tilde{y}(\tilde{x} + \tilde{y})}\end{aligned}\quad (40)$$

The last step follows because recall that for a uniform beam,  $a = 2\tilde{x}$ ,  $b = 2\tilde{y}$ . This can be written as a potential

$$\Phi(x, y) = -\frac{\lambda}{4\pi\epsilon_0} \frac{1}{2(\tilde{x} + \tilde{y})} \left( \frac{x^2}{\tilde{x}} + \frac{y^2}{\tilde{y}} \right) \quad (41)$$

To find the derivation, try *Foundations of Potential Theory* by O. Kellogg. It's tedious, but you can at least simply show that this potential satisfies the Poisson equation  $\nabla^2\Phi = (\lambda/A)/\epsilon_0$ , where  $A = \pi ab$  the ellipse area.

These fields give the linear part of the force.  $F_x = m \frac{d^2x}{dt^2} = mv^2 x'' = 2E_k x'' = 2qV_0 x''$ . ( $V_0$  is the non-relativistic energy per charge,  $E_k/q$  introduced in lecture 3.)

$$x''|_{\text{SC}} = \frac{F_x}{2qV_0} = \frac{\mathcal{E}_x}{2V_0} = \frac{I \times 30 \Omega}{2\beta V_0} \frac{x}{\tilde{x}(\tilde{x} + \tilde{y})} \quad (42)$$

(Remember:  $\frac{\lambda}{4\pi\epsilon_0} = \frac{30\Omega I}{\beta}$ .)

The dimensionless factor  $\frac{2I \times 30 \Omega}{\beta V_0}$  is referred to as the 'generalized perveance'  $K_{\text{perv}}$ , so this can be written as

$$x''|_{\text{SC}} = \frac{K_{\text{perv}}}{4} \frac{x}{\tilde{x}(\tilde{x} + \tilde{y})} \quad (43)$$

(For the  $y$  equation, just swap the  $x$ 's and  $y$ 's.)

### 9.5.2 Envelope equation

We stay with the simple case where the beamline consists only of elements that keep all 3 degrees of freedom independent of each other, and there is only a linear focusing force  $k(s)$  that varies with  $s$ . Moreover,  $k(s)$  contains a component from space charge. In other words, the Hamiltonian is  $P^2/2 + k(s)x^2/2$ , so

$$\mathbf{F} = \begin{pmatrix} 0 & 1 \\ -k & 0 \end{pmatrix}. \quad (44)$$

This can also be demonstrated from  $x' = P$ , and  $P' = -kx$ , or in matrix form,  $\mathbf{X}' = \mathbf{F}\mathbf{X}$ :

$$\begin{pmatrix} x' \\ P' \end{pmatrix} = \begin{pmatrix} 0 & 1 \\ -k & 0 \end{pmatrix} \begin{pmatrix} x \\ P \end{pmatrix}. \quad (45)$$

Plugging  $\mathbf{F}$  into 34, we have

$$\begin{pmatrix} \sigma'_{11} & \sigma'_{12} \\ \sigma'_{12} & \sigma'_{22} \end{pmatrix} = \begin{pmatrix} 2\sigma_{12} & \sigma_{22} - k\sigma_{11} \\ \sigma_{22} - k\sigma_{11} & -2k\sigma_{12} \end{pmatrix}. \quad (46)$$

Combining some,

$$\sigma''_{11} = 2\sigma'_{12} = 2\sigma_{22} - 2k\sigma_{11} \quad (47)$$

The emittance  $\epsilon$  is given by the determinant

$$\epsilon^2 = \sigma_{11}\sigma_{22} - \sigma_{12}^2. \quad (48)$$

It is **constant**. (Exercise: Show this by using eqn. 46 to prove that  $(\epsilon^2)' = 0$ .)

We can eliminate  $\sigma_{22}$ :

$$\sigma''_{11} = 2(\epsilon^2 + \sigma_{12}^2)/\sigma_{11} - 2k\sigma_{11} \quad (49)$$

Now recall the **RMS** size as  $\tilde{x} = \sqrt{\sigma_{11}}$ . Then  $\sigma'_{11} = 2\tilde{x}\tilde{x}'$  so  $\sigma_{12} = \tilde{x}\tilde{x}'$  and  $\sigma''_{11} = 2\tilde{x}\tilde{x}'' + 2\tilde{x}'^2$ . Putting this all together, we get

$$\tilde{x}'' + k\tilde{x} - \frac{\epsilon^2}{\tilde{x}^3} = 0, \quad (50)$$

This is the envelope eqn; looks like the single particle equation except for the emittance term. (Remember:  $\tilde{x}$  is the beam RMS size, not the particle coordinate.)

### 9.5.3 Space Charge Envelope Equations

Let us separate  $k = k_x - \frac{K_{\text{perv}}}{4\tilde{x}(\tilde{x}+\tilde{y})}$  where the former is from externally applied fields of linear lenses, and latter term comes from eqn. 43.

$$\begin{aligned} \tilde{x}'' + k_x\tilde{x} - \frac{K_{\text{perv}}/4}{\tilde{x} + \tilde{y}} - \frac{\epsilon_x^2}{\tilde{x}^3} &= 0 \\ \tilde{y}'' + k_y\tilde{y} - \frac{K_{\text{perv}}/4}{\tilde{x} + \tilde{y}} - \frac{\epsilon_y^2}{\tilde{y}^3} &= 0 \end{aligned} \quad (51)$$

Alternatively, if we let  $a = 2\tilde{x}$ ,  $b = 2\tilde{y}$  then emittances  $\epsilon_a = 4\epsilon_x$ ,  $\epsilon_b = 4\epsilon_y$ :

$$\begin{aligned} a'' + k_x a - \frac{K_{\text{perv}}}{a+b} - \frac{\epsilon_a^2}{a^3} &= 0 \\ b'' + k_y b - \frac{K_{\text{perv}}}{a+b} - \frac{\epsilon_b^2}{b^3} &= 0 \end{aligned} \quad (52)$$

These two are the ‘‘Kapchinsky-Vladimirsky’’ equations.[19]

### 9.5.4 Bunched beams

In  $\mathbf{F}$ -matrix form, the space charge contribution is

$$\mathbf{F}_{\text{sc}} = \begin{pmatrix} 0 & 0 & 0 & 0 & 0 & 0 \\ K_{\text{xsc}} & 0 & 0 & 0 & 0 & 0 \\ 0 & 0 & 0 & 0 & 0 & 0 \\ 0 & 0 & K_{\text{ysc}} & 0 & 0 & 0 \\ 0 & 0 & 0 & 0 & 0 & 0 \\ 0 & 0 & 0 & 0 & 0 & 0 \end{pmatrix} \quad (53)$$

where  $K_{xsc} = \frac{K_{perv}}{a(a+b)}$ ,  $K_{ytc} = \frac{K_{perv}}{b(a+b)}$ . If the beam is in bunches rather than continuous, we need the electric field of an ellipsoidal distribution of charge. It turns out, surprisingly (Sacherer, 1971), that the RMS linear part of the space charge self-field depends mainly on the RMS size of the distribution and only very weakly on its exact form. To within a few percent, the RMS linear part of space charge is the same as that for a uniformly populated ellipsoid. The space charge infinitesimal transfer matrix is

$$\mathbf{F}_{sc} = \begin{pmatrix} 0 & 0 & 0 & 0 & 0 & 0 \\ K_{xsc} & 0 & 0 & 0 & 0 & 0 \\ 0 & 0 & 0 & 0 & 0 & 0 \\ 0 & 0 & K_{ytc} & 0 & 0 & 0 \\ 0 & 0 & 0 & 0 & 0 & 0 \\ 0 & 0 & 0 & 0 & K_{zsc} & 0 \end{pmatrix} \quad (54)$$

where

$$K_{xsc} = \frac{Q}{4\pi\epsilon_0(mc^2/e)\beta^2\gamma^3} \frac{1}{a^3} g\left(\frac{b^2}{a^2}, \frac{c^2}{a^2}\right) \quad (55)$$

$$K_{ytc} = \frac{Q}{4\pi\epsilon_0(mc^2/e)\beta^2\gamma^3} \frac{1}{b^3} g\left(\frac{c^2}{b^2}, \frac{a^2}{b^2}\right) \quad (56)$$

$$K_{zsc} = \frac{Q}{4\pi\epsilon_0(mc^2/e)\beta^2\gamma^3} \frac{1}{c^3} g\left(\frac{a^2}{c^2}, \frac{b^2}{c^2}\right) \quad (57)$$

where  $Q$  is the bunch charge, the ellipsoid semi-axes in the  $x, y, z$  directions are  $a, b, c$ , and the function  $g$  is

$$g(u, v) = \frac{3}{2} \int_0^\infty (1+s)^{-3/2} (u+s)^{-1/2} (v+s)^{-1/2} ds \quad (58)$$

This is from the family of Carlson elliptic integrals.

## 9.6 But space charge is nonlinear... what about arbitrary bunch distributions, orientations

This was thought to be a huge impediment to using envelope formulation for when space charge not negligible.

EUROPEAN ORGANIZATION FOR NUCLEAR RESEARCH

96

CERN/SI/Int. DL/70-12  
18.11.1970RMS ENVELOPE EQUATIONS WITH SPACE CHARGE

Frank J. Sacherer

ABSTRACT

The envelope equations for a continuous beam with circular symmetry but otherwise arbitrary charge distribution have been derived by Lapostolle and Gluckstern. Their results are extended in this report to continuous beams with elliptical symmetry and to bunched beams with ellipsoidal form.

square) values. This results because (i) the second moments of any particle distribution depend only on the linear part of the force (determined by least squares method), while (ii) this linear part of the force in turn depends only on the second moments of the distribution. This is also true in practice for three-dimensional bunched beams with ellipsoidal symmetry, and allows the formulation of envelope equations that include the effect of space charge on bunch length and energy spread.

But there is a surprising property that if the beam is not uniform, as long as we use RMS values, and the distribution has elliptical symmetry  $f(x, y) = f\left(\frac{x^2}{a^2} + \frac{y^2}{b^2}\right)$ , it remains true. This remarkable theorem was discovered and proved by Frank Sacherer (1971).

The only complication is that the RMS emittance is then not guaranteed to be constant. However, for well-designed beamlines, the emittance growth is minimal.

For arbitrary distributions of the type  $f(x, y, z) = f\left(\frac{x^2}{a^2} + \frac{y^2}{b^2} + \frac{z^2}{c^2}\right)$ , replace  $a, b, c$  with the RMS values according to the values they have for the uniform case, namely,

$a^2 = 5\sigma_{11}$ ,  $b^2 = 5\sigma_{33}$ . Because of relativity,  $c^2$  is a special case:  $c^2 = 5\gamma^2\sigma_{55}$ . For arbitrary orientations, have to apply a rotation matrix to  $F$ , thus making  $F_{23}, F_{25}, F_{41}, F_{45}, F_{61}, F_{63}$  also non-zero.

Notice the recursiveness. This is the essential property of space charge: Particle trajectories are **linear** even though the envelopes themselves are **nonlinear**.

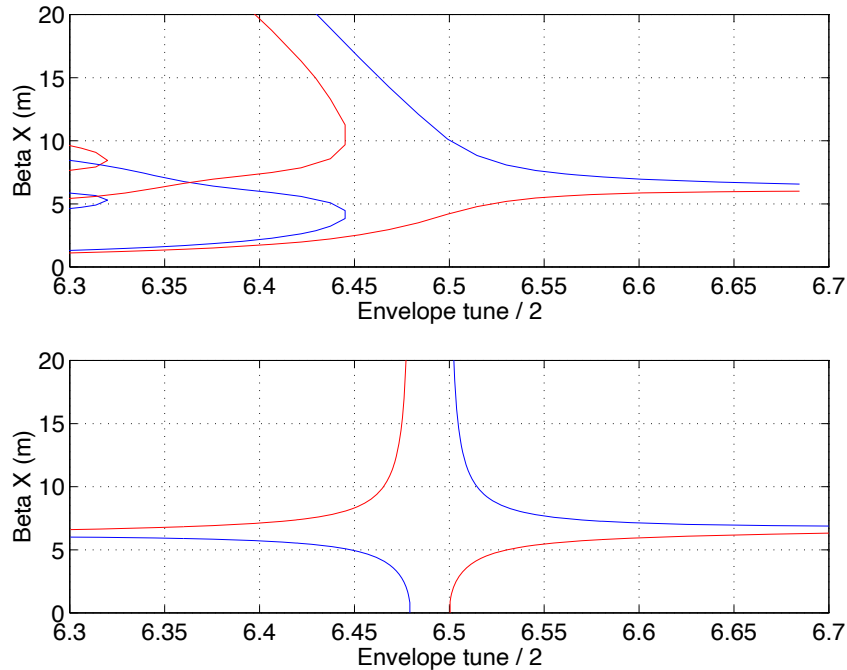
## 9.7 Successfully applied to:

- beamlines, achromatic fitting, space charge
- complex transport problems such as einzel lenses, soft-landing, into solenoid, cyclotron inflectors
- synchrotrons: finding  $\beta$ -functions with space charge, investigating linear coupling and coherent envelope oscillations (half-integer resonances)
- linear accelerators...

As well, it has optimization routines; simplex method, simulated annealing.

### 9.7.1 Example: FNAL Booster

An interesting example is the FNAL booster. First of all, how do we find the optics of a synchrotron? Simple: Launch a  $\sigma$  matrix, integrate around the ring, find how it's changed, allow input  $\sigma$  matrix to vary to fit the final beam to the initial. This gives the (space charge-modified) periodic beta and dispersion functions: animation (or try this one). These weird  $\beta$ -functions can be understood as in the following. Bottom is when they diverge due to an ordinary 13/2 resonance driven by a focusing irregularity. The top is the case when the resonance is approached due to space charge tune depression. This is from paper[21].



For comparison: CSNS multi-particle (pyIMPACT) simulation of similar case.

## 10 Extra dividend from use of equations of motion

There is only a very small subset of elements that are well described by “canned” analytic transfer matrices, and these are highly idealized: solenoids, quadrupoles and dipoles with hard edges, and of course drifts. That’s about it! Cannot do: Quads with soft edges, realistic solenoids, einzel lenses, Ambient Axial Magnetic Field, Arbitrary Axial Electric Field for soft-landing on target, Soft-edge Acceleration Column, Spiral Inflector, Permanent Magnet Axial Lens, RF devices: Bunchers, Linear Accelerator, RFQ. Yes, these are all now in TRANSOPTR.

This methodology allows not only space charge, but any general case with no closed-form solution to equations of motion, e.g. varying axial fields either magnetic or electric as in soft-landing ions into a sample; linear accelerators; short-soft-edge quads;... virtually any element whose Hamiltonian is known.

In fact, for any optics device that is intended to be linear, the procedure for adding it to the code is:

1. Write down the Hamiltonian for Frenet-Serret frame.
2. Expand to quadratic order (there should not be any linear terms, why?).
3. Find the  $\mathbf{F}$ -matrix, and code it in.

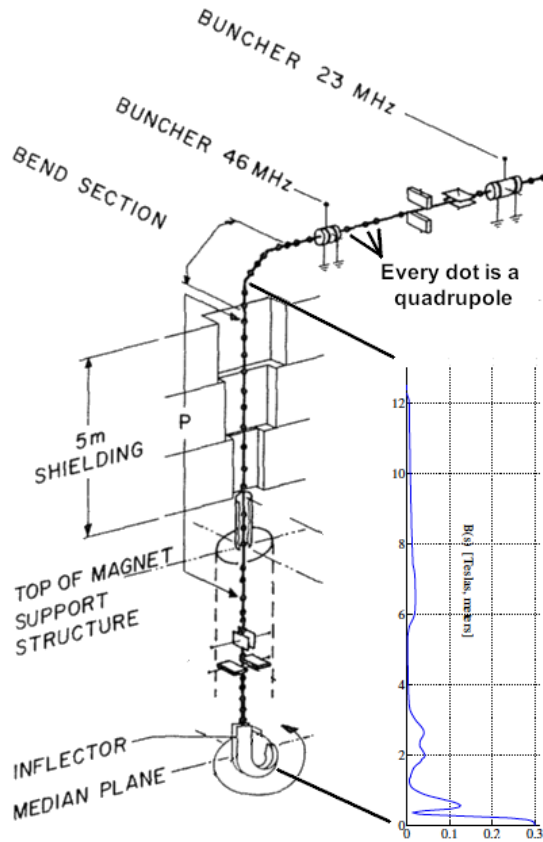
## 11 Example: Cyclotron injection line

After 37 years of operation, we needed to replace the 13 metre, 300 keV vertical section of the injection line into the cyclotron. All optics in this line are electrostatic, and the insulators were becoming conductive with accumulated deposits. This line has everything: a bunching beam with strong space charge (5 mA peak), a varying axial solenoid field, and finally a spiral inflector: a device that strongly couples are phase space variables. We did not want to reproduce the existing line, which performed poorly and contained features we no longer needed. It consists of a FODO periodic section of about 10 meters and 10 periods, and a matching section that has to accommodate various levels of space charge and match to a pathologically-coupled device, the spiral inflector.



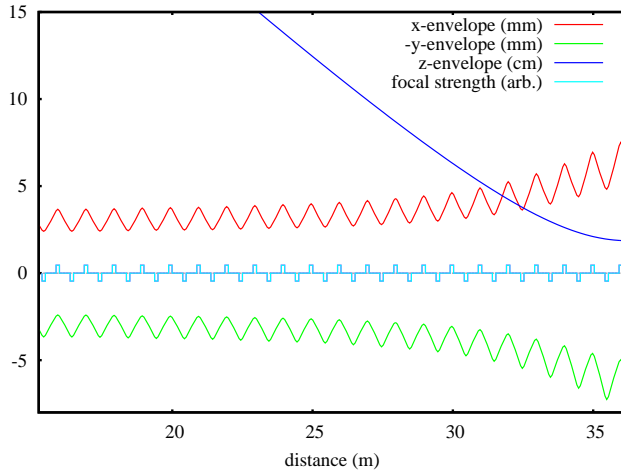
The wide range of conditions requires millions of simulations while varying quad lengths, strengths, orientations, and locations. Multiparticle is impractical here. Instead all calculations were made using TRANSOPTR; not a single multi-particle simulation was run. Yet, it operated as soon as we turned it on in 2011, at theoretical quadrupole settings, and has run ever since. Reminder: as all optics is electrostatic, and internal to the vacuum chamber, a local spill of as little as 1% can melt electrodes.

### 11.1 As built (1974~2011)



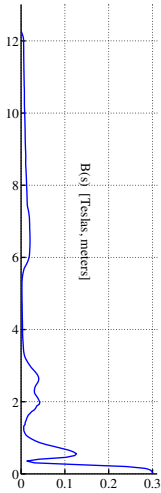
### 11.2 Bunching into a $36^\circ$ phase acceptance

Ignore the details of 2-harmonic bunching, take only the linear part. I.e. launch the beam at buncher with a negative correlation between phase and energy.  $r_{56} = -1$ ,  $\sqrt{5}\sigma_{55} = \beta\lambda/2$ , and  $\sqrt{5}\sigma_{66} \propto V_{\text{buncher}}$  optimized to give minimum bunch length at injection gap.



Test calculation of bunching beam in a periodic section. Final bunch is 12 mm dia. by 34 mm long. ( $\beta\lambda = 329$  mm at 23 MHz, so this is roughly the  $36^\circ$  desired.)

### 11.3 Strong $x$ - $y$ coupling due to axial field



$$F_{\text{axial}B} = \begin{pmatrix} 0 & 1 & \frac{-1}{2\rho(s)} & 0 & 0 & 0 \\ \frac{-1}{4\rho(s)^2} & 0 & 0 & \frac{-1}{2\rho(s)} & 0 & 0 \\ \frac{1}{2\rho(s)} & 0 & 0 & 1 & 0 & 0 \\ 0 & \frac{1}{2\rho(s)} & \frac{-1}{4\rho(s)^2} & 0 & 0 & 0 \\ 0 & 0 & 0 & 0 & 0 & 1 \\ 0 & 0 & 0 & 0 & 0 & 0 \end{pmatrix} \quad (59)$$

which arises from the solenoid Hamiltonian

$$H_{\text{axial}B} = \frac{1}{2} \left( P_x - \frac{y}{2\rho(s)} \right)^2 + \frac{1}{2} \left( P_y + \frac{x}{2\rho(s)} \right)^2 + \frac{1}{2} P_z^2, \quad (60)$$

where  $1/\rho(s) = B(s)/(B\rho)$ , is a function of the independent variable  $s$ . Interpolate it using cubic spline.

### 11.4 Strong $x$ - $y$ - $z$ coupling in the inflector

(See *A Canonical Treatment of the Spiral Inflector for Cyclotrons* Baartman and Kleeven, Part. Acc. **41** (1993).)

$$H(x, y, z, P_x, P_y, P_z; s) = \quad (61)$$

$$\frac{1}{2} \left[ \left( P_x + \frac{TC}{A} y \right)^2 + \left( P_y - \frac{TC}{A} x \right)^2 + \left( P_z + \frac{2TS}{A} y + \frac{2}{A} x \right)^2 \right]$$

$$- \frac{1}{2A^2} \left[ \xi (x + k'Sy)^2 + x^2 + kk'(C^2 x^2 + y^2) + 2TSxy \right].$$

where

$$\xi = \frac{1 + kk'S^2}{1 + k'^2 S^2}, \quad S = \sin(s/A), \quad C = \cos(s/A), \quad T = \frac{k + k'}{2}, \quad k = \frac{A}{\rho} + k',$$

$A$  is electric radius,  $\rho = \rho(s)$  is magnetic radius,  $k'$  is tilt parameter.

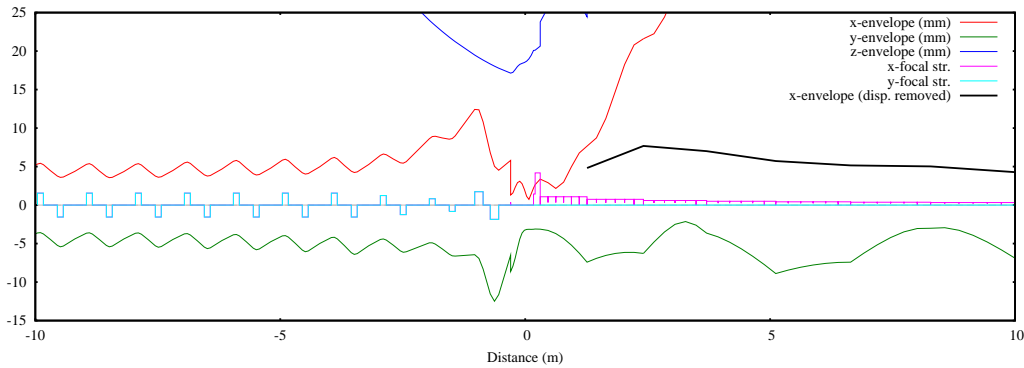
### 11.5 inflector matrix

$$F_{\text{inflector}} = \begin{pmatrix} 0 & 1 & \frac{TC}{A} & 0 & 0 & 0 \\ \frac{3-\xi+(T^2-kk')C^2}{-A^2} & 0 & \frac{3TS-k'\xi S}{-A^2} & \frac{TC}{A} & 0 & \frac{-2}{A} \\ \frac{-TC}{A} & 0 & 0 & 1 & 0 & 0 \\ \frac{3TS-k'\xi S}{-A^2} & \frac{-TC}{A} & \frac{(1+3S^2)T^2-kk'-k'^2\xi S^2}{-A^2} & 0 & 0 & \frac{-2TS}{A} \\ \frac{2}{A} & 0 & \frac{2TS}{A} & 0 & 0 & 1 \\ 0 & 0 & 0 & 0 & 0 & 0 \end{pmatrix}. \tag{62}$$

BTW, if integrated with no space charge, this gives matrix that agrees with other codes (CASINO, AXORB).

The inflector is followed by a deflector: crossed  $E$  and  $B$  fields so looks like a Wien filter.

### 11.6 Injection Matching Detail



## 12 The original sin of TRANSPORT (what are the canonical variables?)

I'll cover the specific case of the linear accelerator, but first, we have to clarify something:

TRANSPORT (and many other codes since) use incorrect longitudinal variables and these prohibit proper calculation of accelerated beams. SLAC-91 (Karl Brown[22]) mentions "At any position in the system... ". This means that time  $t$  is **NOT** the independent variable. Then goes on: "...particle represented by a vector":

$$(x, \theta, y, \phi, l, \delta)$$

(where  $l$  is trajectory length and  $\delta \equiv \Delta P/P$ ).

This is **wrong**: The canonical pair are  $(t - t_0, E - E_0)$  or  $(\Delta t, \Delta E)$ , **not**  $(l, \Delta P/P)$ .

The reason it works usually is by applying a trick: If we scale by  $\beta c$ , we can make them agree, since  $\beta c \Delta t = z$ ,  $\Delta E/(\beta c) = \Delta P$ , but **only true of static magnetic elements**: Electric potential  $\Phi = 0$ ,  $\vec{A} \neq \vec{A}(t)$ .

Mathematical Formulation of TRANSPORT(\*)

The following of a charged particle through a system of magnetic lenses may be reduced to a process of matrix multiplication. At any specified position in the system an arbitrary charged particle is represented by a vector (single column matrix),  $X$ , whose components are the positions, angles, and momentum of the particle with respect to a specified reference trajectory.

$$\text{i. e. } X = \begin{bmatrix} x \\ \theta \\ y \\ \phi \\ l \\ \delta \end{bmatrix}$$

Definitions:

- $x$  = the radial displacement of the arbitrary ray with respect to the assumed central trajectory.
- $\theta$  = the angle this ray makes in the radial plane with respect to the assumed central trajectory.
- $y$  = the transverse displacement of the ray with respect to the assumed central trajectory.
- $\phi$  = the transverse angle of the ray with respect to the assumed central trajectory.

(\*) For a more complete description of the mathematical basis of TRANSPORT, refer to SLAC Report 75, the Appendix of this report and to other References listed at the end of this report.

$l$  = the path length difference between the arbitrary ray and the central trajectory

$\delta = \Delta P/P$  is the fractional momentum deviation of the ray from the assumed central trajectory.

The magnetic lens is represented by a square matrix,  $R$ , which describes the action of the magnet on the particle coordinates. Thus the passage of a charged particle through the system may be represented by the equation:

$$X [1] = R X [0] \tag{1}$$

where  $X [0]$  is the initial coordinate vector and  $X [1]$  is the final coordinate vector of the particle under consideration;  $R$  is the transformation matrix for all such particles traversing the system (one particle differing from another only by its initial coordinate vector  $X [0]$ ).

The traversing of several magnets and interspersing drift spaces is described by the same basic equation but with  $R$  now being the product matrix  $R = R(n) \dots R(3)R(2)R(1)$  of the individual matrices of the system elements. The following of a charged particle via TRANSPORT through a system of magnets is thus analogous to tracing rays through a system of optical lenses except that TRANSPORT is a matrix calculation which truncates the problem to either first or second-order in a Taylor's expansion about a central trajectory. For studying beam optics to greater precision than a second-order TRANSPORT calculation permits,

Table 2: Various codes and their longitudinal coordinate definitions. The fifth column (EoM?) refers to whether the equations of motion are integrated as opposed to having stored transfer matrices. The rightmost column refers to whether the reference particle can be accelerated within an element. ( $K \equiv (\gamma_0 - 1)mc^2$ ,  $\Delta t \equiv t - t_0$ )

code	Order	$x_5$	$x_6$	Canonical?	EoM?	$\beta_0(s)?$
TRANSPORT[23]	up to 3	$-(\beta ct - \beta_0 ct_0)$	$\frac{\Delta P}{P_0}$	No	No	–
GIOS[24]	3	$\frac{\Delta t}{t_0}$	$\frac{\Delta E}{K}$	No	No	–
TRACE3D[25]	1	$-\beta_0 c \Delta t$	$\frac{\Delta P}{P_0}$	No	No	impulses
COSY- $\infty$ [26]	$\infty$	$-\frac{\beta_0 c \Delta t \gamma_0}{1 + \gamma_0}$	$\frac{\Delta E}{K}$	Yes	Yes	No
MARYLIE[27]	3	$-c \Delta t$	$\frac{\Delta E}{P_0 c}$	Yes	Yes	No
TRANSOPTR[28]	1	$-\beta_0 c \Delta t$	$\frac{\Delta E}{\beta_0 c}$	Yes	Yes	Yes

## 13 Linac:

This includes any rf gap, bunchers, multi-gap DTL tanks, elliptical electron cavities, etc. Anything symmetric, all that is needed is an interpolatable axial electric field.

Here is the Hamiltonian for the distance along the reference trajectory  $s$  as the independent variable,

$$\begin{aligned}
 H(x, P_x, y, P_y, t, E; s) &= \\
 &= -qA_s - \sqrt{\left(\frac{E - q\Phi}{c}\right)^2 - m^2 c^2 - (P_x - qA_x)^2 - (P_y - qA_y)^2}
 \end{aligned} \tag{63}$$

### 13.1 Potentials

The case of RF axially-symmetric electric field can be handled entirely with no electric potential ( $\Phi = 0$ ), and time-varying vector potential. This has been presented a number of times in the past (e.g. E.E. Chambers;1968[29]), but we are interested in the following more experimentally-useful case: The electric field along the axis  $\mathcal{E}(s)$  has been measured and is therefore known, and the geometry is exactly axially symmetric.

For a gauge that zeroes both  $A_x$  and  $A_y$ , the potentials are

$$A_x = 0, \quad A_y = 0, \quad A_s = -\mathcal{E}(s) \left( 1 - \frac{\omega^2 x^2 + y^2}{c^2} \right) \frac{\sin(\omega t + \theta)}{\omega} \quad (64)$$

and scalar potential:

$$\Phi = -\frac{\partial \Psi}{\partial t} = \mathcal{E}' \cos(\omega t + \theta) \frac{x^2 + y^2}{4} \quad (65)$$

Now if we expand the Hamiltonian, we get:

$$\begin{aligned} H(x, P_x, y, P_y, z, P_z; s) &= \frac{P_x^2}{2P} + \frac{P_y^2}{2P} + \frac{q}{2\beta c} \left( \mathcal{E}' C - \mathcal{E} S \frac{\omega\beta}{c} \right) \frac{r^2}{2} + \\ &\quad \frac{P_z^2}{2\gamma^2 P} + \frac{q\mathcal{E}C}{\beta c} \frac{zP_z}{\gamma^2 P} - \frac{q\mathcal{E}\omega S}{\beta^2 c^2} \frac{z^2}{2} \end{aligned} \quad (66)$$

( $C \equiv \cos(\omega t_0(s) + \theta)$ ,  $S \equiv \sin(\omega t_0(s) + \theta)$ ) This has nice intuitive explanations for the individual terms. (1) The factor in parentheses represents usual the focal power of an RF gap, e.g. a buncher. (2) Taking the limit as  $\omega \rightarrow 0$  reproduces precisely the Hamiltonian of the DC accelerator. Note that in that case,  $\mathcal{E}' = -\phi''$ .

## 13.2 Infinitesimal Transfer Matrix F

Now that the Hamiltonian for linear motion (eqn.66) has been obtained, it is a simple matter to find the infinitesimal transfer matrix  $F$ . Writing the equations of motion ( $x' = \partial H / \partial P_x$ ,  $P'_x = -\partial H / \partial x$ , etc.), the following  $F$ -matrix is found for the axially symmetric linear accelerator:

$$F = \begin{pmatrix} 0 & \frac{1}{P} & 0 & 0 & 0 & 0 \\ \mathcal{A}(s) & 0 & 0 & 0 & 0 & 0 \\ 0 & 0 & 0 & \frac{1}{P} & 0 & 0 \\ 0 & 0 & \mathcal{A}(s) & 0 & 0 & 0 \\ 0 & 0 & 0 & 0 & \frac{\beta'}{\beta} & \frac{1}{\gamma^2 P} \\ 0 & 0 & 0 & 0 & \mathcal{B}(s) & -\frac{\beta'}{\beta} \end{pmatrix}. \quad (67)$$

where we have defined:

$$\mathcal{A}(s) = \frac{-q}{2\beta c} \left( \mathcal{E}' C - \mathcal{E} S \frac{\omega\beta}{c} \right), \quad \mathcal{B}(s) = \frac{q\mathcal{E}\omega S}{\beta^2 c^2}. \quad (68)$$

But:

- **F**-matrix is now a function of time as well as  $s$ ,
- Energy is changing so
- Therefore, time and energy of the reference particle not known a priori anymore: they must be calculated by separate integrals.

This means there are 2 more equations of motion besides the 21 for the  $\sigma$  matrix.[30] A priori, we do not know the reference particle's energy and time coordinates. We need these in order to expand about them. (See eqn. 35.) They can be found from the equations of motion evaluated at  $x = y = P_x = P_y = 0$ :

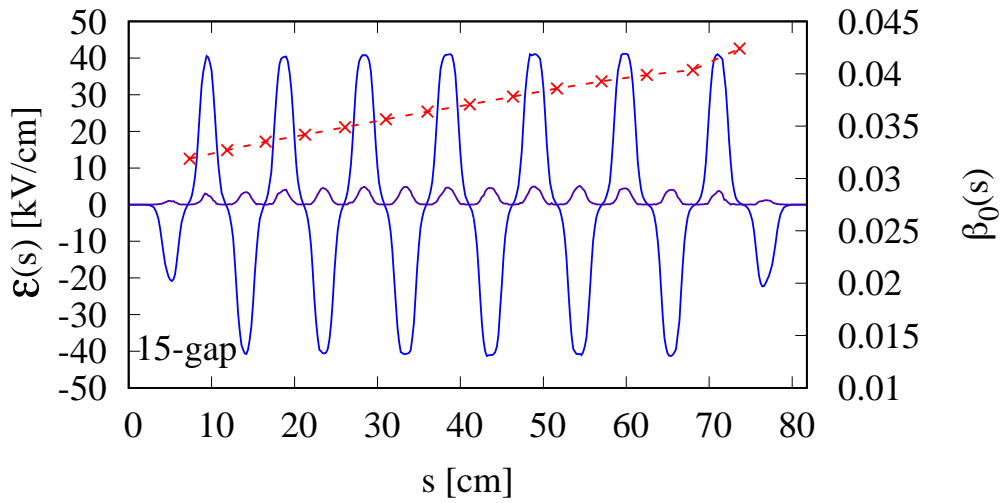
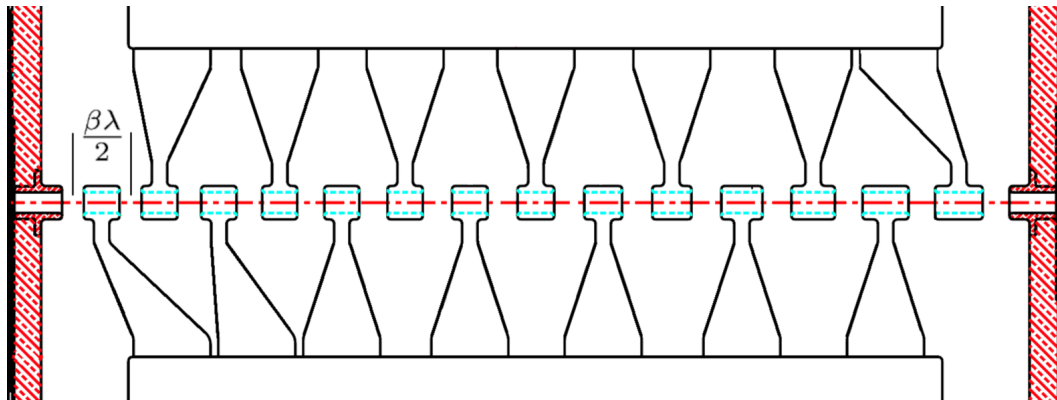
$$\frac{dE_0}{ds} = \frac{\partial H}{\partial t} = q\mathcal{E} \cos(\omega t_0 + \theta) \quad (69)$$

$$\frac{dt_0}{ds} = -\frac{\partial H}{\partial E} = \frac{E_0}{P_0} = \frac{1}{\beta_0 c} \quad (70)$$

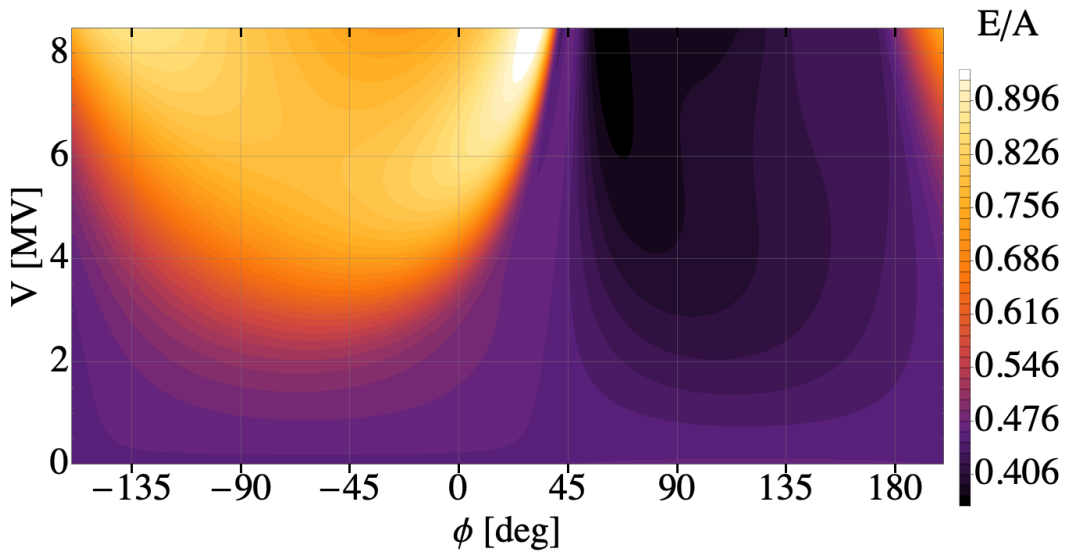
These 2 are added to the 21 mentioned previously; 23 solved together.[30]

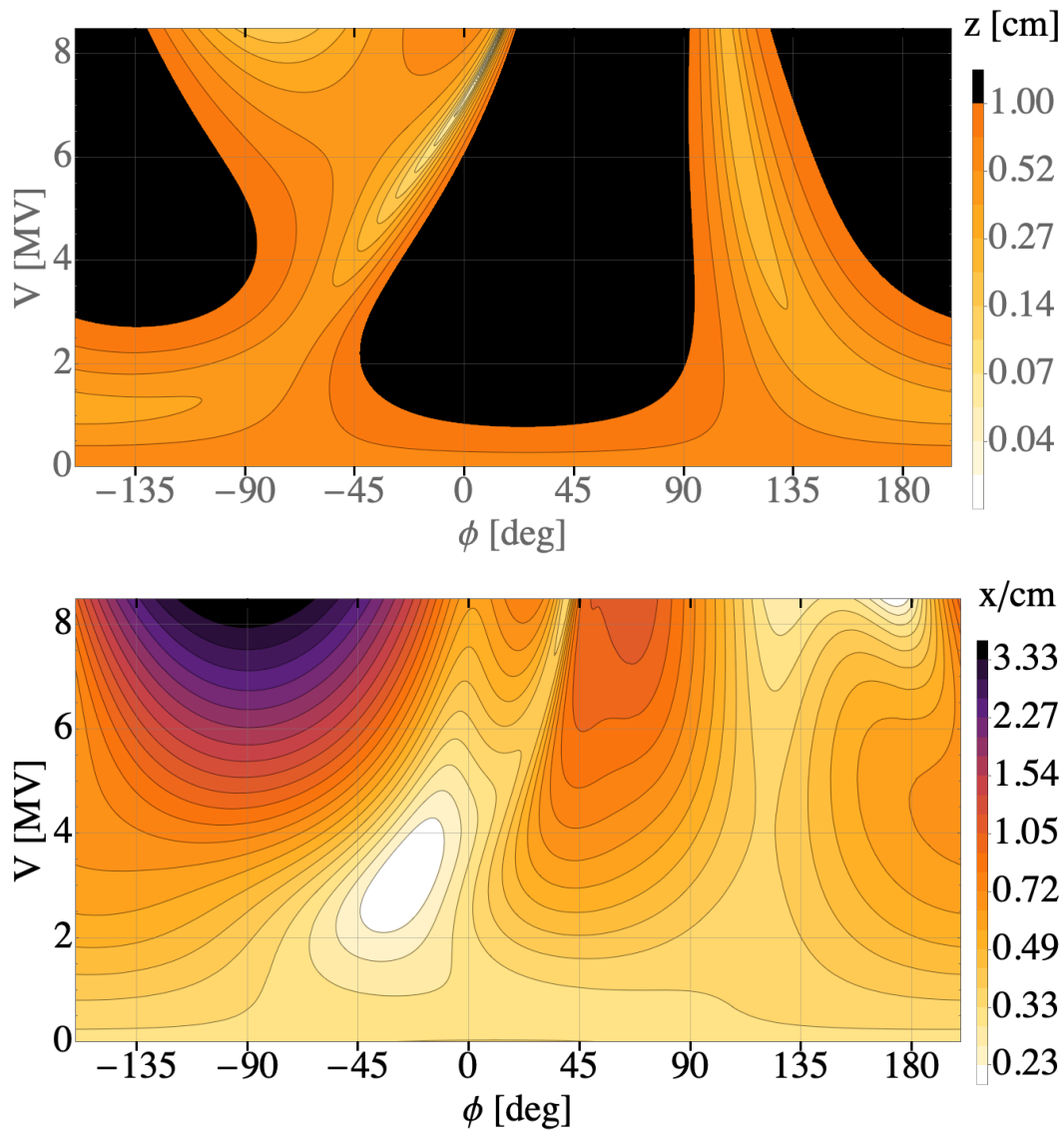
### 13.3 Example: ISAC DTL

Here's an example of what you can do with a fast code: Find all possible combinations of phase and amplitude on a 15-gap DTL designed for accelerating heavy ions.



This particular tank, accelerates ions from 0.46 MeV/u to 0.78 MeV/u. ( $\beta = 3.1\%$  to 4.1%) The frequency is 105 MHz so  $\beta\lambda = 9.0$  cm at start and 11.7 cm at the exit.

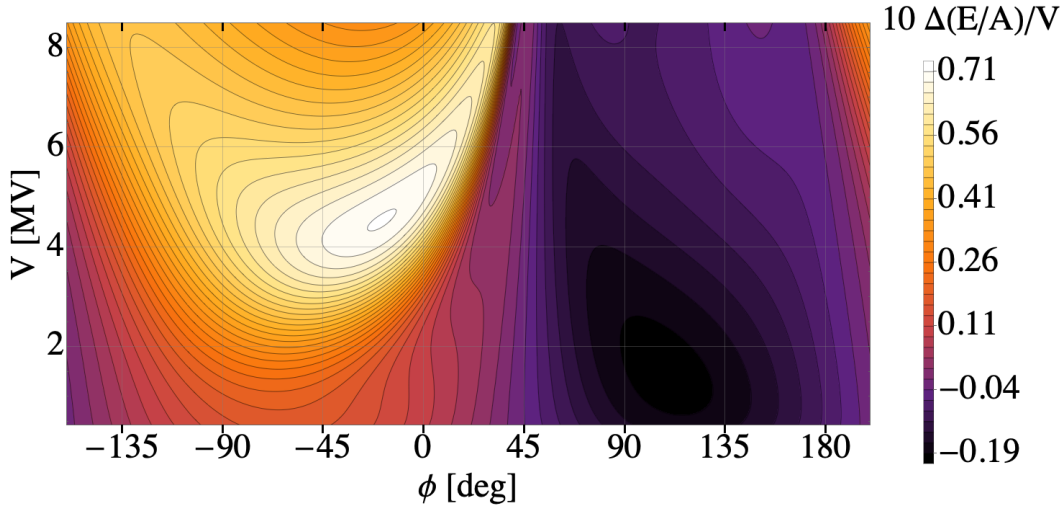




Plots are from a single calculation of half a million runs through the DTL, that took a few hours to run.

Reminder: TRANSOPTR can only do linear optics, so if bunch is too long, it will “banana” due to the rf nonlinearity. The black areas are for bunches of half-length longer than 1 cm, i.e. bunches extending over a length of greater than  $80^\circ$ . The preferred path is the light colour, typically one tenth this length.

The design operating condition is the centre of the white island in the following plot, where the energy gain has been divided by the rf amplitude:



## 14 RFQ:

Not satisfied with axially symmetric linacs, we've also coded an RFQ, where  $x$  and  $y$  focusing have opposite signs. Interesting and subtle difference in that spatial phase must be tracked.[31]

### 14.1 Hamiltonian Dynamics

In an RFQ, the fields are electric and the magnetic forces are negligible. It is therefore possible to analyze it with only a time-varying scalar potential. Then with the independent variable is  $s$ , the distance along the path taken by the reference particle, the Hamiltonian is  $-P_s$ , the canonical momentum in the direction of the reference trajectory.

$$H_s(x, P_x, y, P_y, t, E; s) = -\sqrt{(E - q\Phi)^2 / c^2 - m^2 c^2 - P_x^2 - P_y^2} \quad (71)$$

### 14.2 RFQ Spatial Phase

We confine ourselves to the simplest, 'two-term' scalar potential for the RFQ (e.g. Wangler[32], Staples[33])

$$\Phi(x, y, s, t) = \frac{V_0}{2} \left( A_{10} \cos(ks) I_0(kr) + A_{01} (x^2 - y^2) \right) \sin(\omega t + \phi), \quad (72)$$

where  $I_0$  is the modified Bessel function and  $r^2 = x^2 + y^2$ . The potential features both the accelerating and focusing efficiencies, respectively defined as:

$$A_{10} = \frac{m^2 - 1}{m^2 I_0(ka) + I_0(mka)} \quad (73)$$

$$A_{01} = \frac{1 - A_{10} I_0(ka)}{a^2} \quad (74)$$

The parameters  $k$ ,  $A_{10}$ ,  $A_{01}$  are usually tabulated, one value per halfcell, versus  $s$ . This potential is used in codes such as PARMTEQ and TRACE3D which calculate through only one halfcell at a time. In that case  $s$  would be reset to zero at each halfcell start. But we would like the ODE solver to run  $s$  from the beginning of the RFQ to its exit, choosing its own stepsize for accuracy and efficiency, while spline-interpolating the three parameters  $k$ ,  $A_{10}$ ,  $A_{01}$ . Thus equation 72 is incorrect for non-piecewise constant values of  $k$  and  $s$  not re-starting at every piece: the spatial modulation to the point  $s$  is not  $ks$  but  $\int_0^s k(\zeta) d\zeta$ .

In a perfect RFQ,  $k(s) = \frac{2\pi}{\beta(s)\lambda} = \frac{\omega}{\beta c} = \omega \frac{dt}{ds}$ , or  $k(s) ds = \omega dt$ , we integrate, arbitrarily using the initial condition  $s = 0$  at  $t = 0$  to define phase, and find  $\int_0^s k(\zeta) d\zeta = \omega t$ . In other words, as time  $t$  progresses, the particle experiencing the potential (72) will not stay synchronous unless the argument of the cosine is

$$\psi(s) = \int_0^s k(\zeta) d\zeta \quad (75)$$

rather than  $ks$ :

$$\Phi(x, y, s, t) = \frac{V_0}{2} \left( A_{10} \cos \psi I_0(kr) + A_{01} (x^2 - y^2) \right) \sin(\omega t + \phi) \quad (76)$$

### 14.3 The On-Axis Reference Particle

In order to transform from  $(t, E)$  to  $(z, P_z) = (-\beta_0(s)c\Delta t, \Delta E/(\beta_0(s)c))$ , we need to first find time  $t_0$  and energy  $E_0$  of the reference particle. We find time  $t_0$  from eqn. (71) as:

$$\frac{dt_0}{ds} = -\frac{\partial H}{\partial E} = \frac{E_0 - q\Phi}{c\sqrt{(E_0 - q\Phi)^2 - m^2 c^4}} = \frac{\gamma}{c\sqrt{\gamma^2 - 1}} = \frac{1}{\beta c}. \quad (77)$$

(This is essentially the definition of  $\beta$  and  $\gamma$ ; from here on, unsubscripted  $\beta$  and  $\gamma$  refer to the reference particle and both are functions of  $s$ .)

We find the energy of the on-axis reference particle now as follows:

$$\frac{dE_0}{ds} = \frac{\partial H}{\partial t} = \frac{1}{\beta c} \frac{\partial \Phi}{\partial t} \quad (78)$$

As above, energy  $E_0$  is not directly  $\gamma mc^2$  because the scalar potential in an RFQ is not zero on axis. In fact,  $\gamma mc^2 = E_0 - q\Phi$ , so:

$$mc^2 \gamma' = \frac{d(E_0 - q\Phi)}{ds} = \frac{1}{\beta c} \frac{\partial \Phi}{\partial t} - q \left( \frac{\partial \Phi}{\partial s} + \frac{\partial \Phi}{\partial t} \frac{dt}{ds} \right) = -q \frac{\partial \Phi}{\partial s} \quad (79)$$

This can be identified as the longitudinal electric field. Performing the derivative of eqn. (76) above for on-axis,

$$mc^2\gamma' = \frac{qV_0}{2}kA_{10} \sin \psi \sin(\omega t_0 + \phi_s), \quad (80)$$

and this agrees with standard references[32], except that the argument of the sine function is  $\psi$  rather than  $ks$ .

#### 14.4 Hamiltonian in $(z, P_z)$

This follows the technique developed for the axially symmetric linac[34]. The Hamiltonian (71) with the potential (76) is transformed to new longitudinal coordinates

$$z = -\beta(s)c(t - t_0(s)) \quad \text{and} \quad P_z = \frac{E - E_0(s)}{\beta(s)c}, \quad (81)$$

where  $t_0(s) = \int \frac{ds}{\beta c}$ . The transformation is most easily understood if done in two steps: first transforming from  $(t, -E)$  to  $(-\Delta t, \Delta E)$ . The generating function that accomplishes this is [35]:

$$G_1 = -\left(t - \int \frac{ds}{\beta c}\right)(\Delta E + E_0) \quad (82)$$

This produces the Hamiltonian-added terms:

$$\frac{\partial G_1}{\partial s} = \frac{\Delta E + E_0(s)}{\beta c} - \Delta t E_0' \quad (83)$$

Next, we transform once more from  $(-\Delta t, \Delta E)$  to  $(-\beta c \Delta t, \Delta E/(\beta c))$ , accomplished by using a second generating function [35]:

$$G_2 = -\beta c \Delta t P_z, \quad (84)$$

thus adding

$$\frac{\partial G_2}{\partial s} = \frac{\beta'}{\beta} z P_z = \frac{\gamma'}{\beta^2 \gamma^3} z P_z \quad (85)$$

to the Hamiltonian (71).

#### 14.5 Hamiltonian for Linear motion

We then substitute eqn. (81) into the Hamiltonian. Since we are only interested in the linear motion, we expand the resulting Hamiltonian to second order in the 6 canonical variables (using the abbreviation  $P \equiv \beta \gamma mc$ ):

$$H(x, P_x, y, P_y, z, P_z) = \frac{E_0}{\beta c} - P + \frac{P_x^2}{2P} + \frac{P_y^2}{2P} + \frac{P_z^2}{2\gamma^2 P} + \frac{\mathcal{A}_+}{2} x^2 + \frac{\mathcal{A}_-}{2} y^2 + \frac{\mathcal{C}}{2} z^2 + \mathcal{B} z P_z \quad (86)$$

where

$$\mathcal{A}_{\pm} = \frac{qV_0 \sin(\omega t_0 + \phi) (k^2 A_{10} \cos \psi \pm 4A_{01})}{4\beta c}, \quad (87)$$

$$\mathcal{B} = \frac{qV_0 A_{10} (k \sin \psi \sin(\omega t_0 + \phi) + (\omega/(\beta c)) \cos \psi \cos(\omega t_0 + \phi))}{2\beta^2 \gamma^3 m c^2}, \quad (88)$$

$$\mathcal{C} = \frac{qV_0 (\omega/(\beta c))^2 A_{10} \cos \psi (qV_0 A_{10}/(\beta^2 \gamma^3 m c^2) \cos \psi \cos^2(\omega t_0 + \phi) - 2 \sin(\omega t_0 + \phi))}{4\beta c} \quad (89)$$

There are no terms first order in the six dependent coordinates, confirming that the reference particle's coordinates are invariant.

## 14.6 Implementation in TRANSOPTR

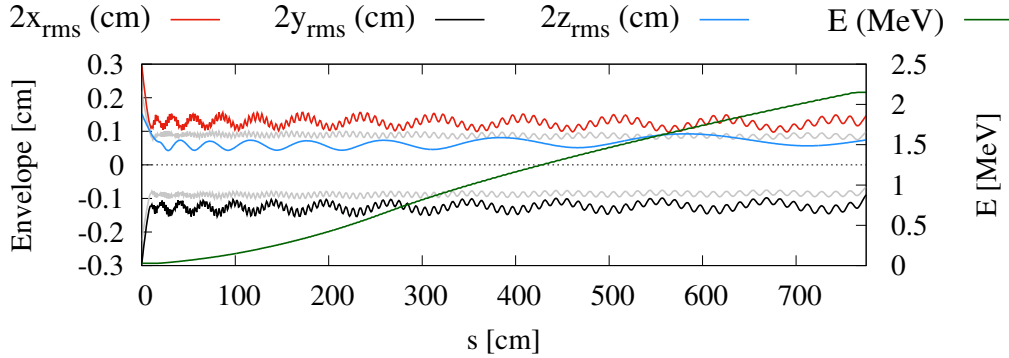
From the Hamiltonian (86) we find directly the  $\mathbf{F}$ -matrix:

$$\mathbf{F} = \begin{pmatrix} 0 & \frac{1}{P} & 0 & 0 & 0 & 0 \\ -\mathcal{A}_+ & 0 & 0 & 0 & 0 & 0 \\ 0 & 0 & 0 & \frac{1}{P} & 0 & 0 \\ 0 & 0 & -\mathcal{A}_- & 0 & 0 & 0 \\ 0 & 0 & 0 & 0 & \mathcal{B} & \frac{1}{\gamma^2 P} \\ 0 & 0 & 0 & 0 & -\mathcal{C} & -\mathcal{B} \end{pmatrix} \quad (90)$$

For the full 6D case, it represents 21 equations (the  $\sigma$ -matrix is symmetric), but in the present case 12 of these are trivial because there is no coupling between the 3 planes. A Runge-Kutta integrator is used to solve eqn. ??, simultaneously while integrating  $\psi' = k$  (75),  $t'_0$  (77), and  $\gamma'$  (80). Space charge is included if needed by augmenting the  $\mathbf{F}$ -matrix with the appropriate linear space charge defocusing terms[36, 34].

In TRANSOPTR a global input data file contains beam initial parameters plus the element parameters one is free to vary. A subroutine describing the transport system optical elements (quads, drifts, solenoids, linacs, etc.) are called in order, or in do loops if they are periodic. The RFQ element is called via the new subroutine RFQ which reads the file containing the table of  $(s, A_{01}, A_{10}, k)$ , and has as arguments the phase and amplitude of the RFQ, and a length scale.

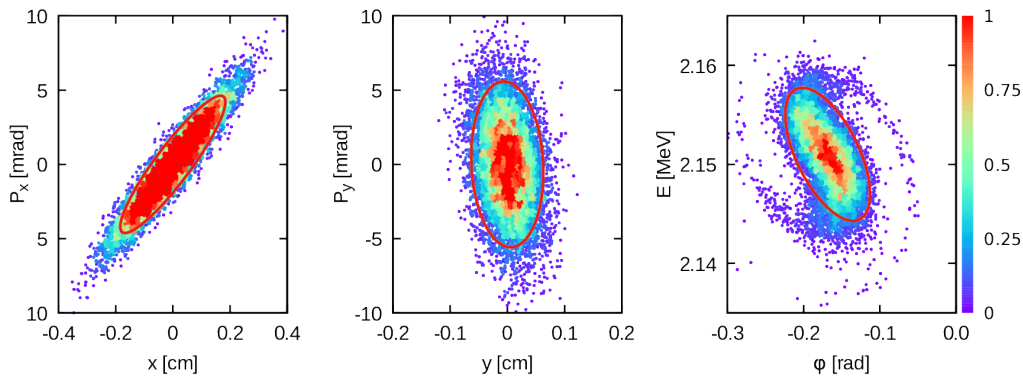
### 14.7 TRIUMF's RFQ



2-term TRANSOPTR simulation of the ISAC-RFQ, showing two times rms envelopes on the left-hand vertical axis, with the  $y$ -envelopes shown as negative values for clarity. The simulation runs from the start of the RFQ tank at  $s = 0$ . Two separate envelopes are shown, corresponding to a matched and a mismatched case, in the transverse dimensions. The mismatched case highlighting the betatron oscillation is shown in color including the longitudinal envelope. The beam energy is shown on the right-hand vertical axis. The transversely matched envelope is shown in light grey.

We've also run the CERN Linac-4 RFQ case, without and with space charge. The former takes 30,000 RK steps, and 131 ms on my Mac, the latter with 35 mA (100 pC per bunch) takes 146 ms.

### 14.8 Comparison to PARMTEQ

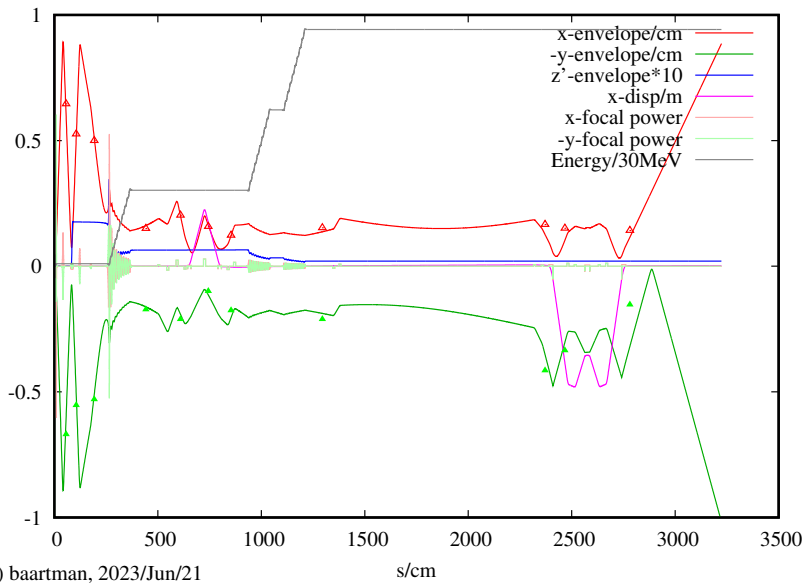


PARMTEQ normalized particle density distribution compared to TRANSOPTR ellipse of area  $4\pi\epsilon_{rms}$ , corresponding to 86% containment for Gaussian distributed beam. Profiles for  $x$ - $P_x$ ,  $y$ - $P_y$  and  $t$ - $E$ , taken at the RFQ vacuum tank exit, 15.83 cm downstream of the vanes.

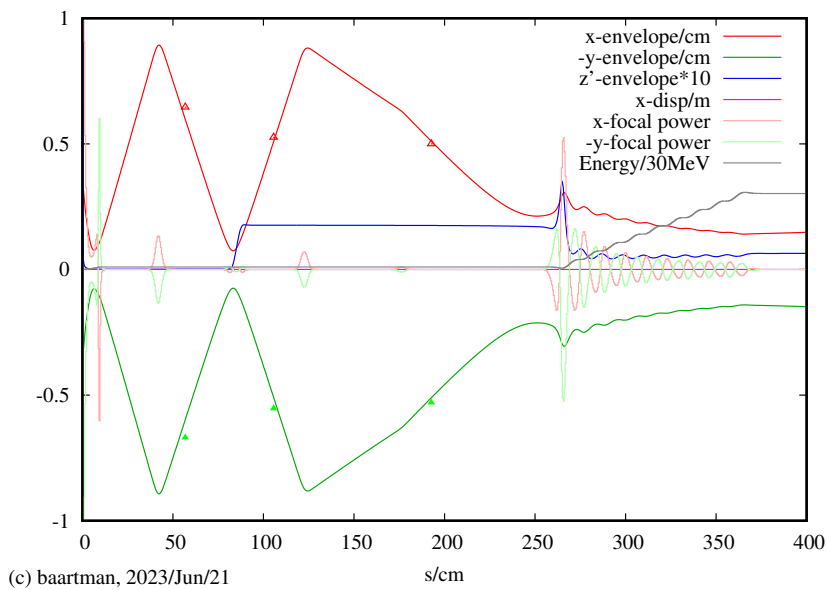
## 15 Application examples

### 15.1 elinac

We have fitted the initial beam right at the cathode, where initially beam energy is 20 eV, and energy spread is 14% and divergence is  $\sim 1$  radian.



Here's a closer look at the starting gun... 3 solenoids, buncher, injector linac:



## 15.2 OLIS steering training for the Bayesian optimization

See animation (or try this one).

## 15.3 MCAT

Model-Coupled Accelerator Tuning intended to sequentially optimize a transport and/or accelerator string, using the TRANSOPTR model.



## 16 Conclusions

Envelope calculations (TRANSOPTR) are most efficient for linear optics with space charge and/or any time the focal parameters vary with  $s$  and no closed-form matrix is possible. Calculations are orders of magnitude faster than multi-particle simulations.

- Beamlines, including minimizing aberrations, can be rapidly designed.
- On-the-fly tuning/optimization is possible in control rooms, even with space charge. This is useful to correct for failed hardware, e.g. as a cavity quenches.
- All aspects of the linear behaviour, including linear coupling, envelope oscillations (half-integer resonances).

Not good for

- Designing higher order corrections, such as required for spectrometers and separators.
- Simulating anything inherently nonlinear. Examples are bunching a DC beam, bunch deformation due to sinusoidal rf waveform.
- Collimation, High intensity beam losses due to halo.

## 17 Acknowledgements

Many people contributed to the applications. Some in my group, some not. Out-of-date pic (missing: HuiWen Koay, Philippe Bélanger, Aveen Mahon, Lige Zhang, Dobrin Kaltchev):



## References

- [1] H. Wollnik, J. Heuser, T. Matsuo, E. Kassekert, K. Becker, J. Brezina, C. Geisse, K. Lindemann, S. Meuser, J. Larson, and J. Troetscher, “Manual for GIOS,” tech. rep., II. Physikalisches Institut, Justus-Leibig-Universitaet, Giessen, F.R.G., July 1988.
- [2] J. Irwin and C.-x. Wang, “Explicit soft fringe maps of a quadrupole,” in

- Proceedings Particle Accelerator Conference*, vol. 4, pp. 2376–2378, IEEE, 1995.
- [3] M. Berz, “Computational aspects of optics design and simulation: COSY INFINITY,” *Nucl. Inst. and Meth. A*, vol. 298, no. 1-3, pp. 473–479, 1990.
- [4] J. Back, J. Pozimski, P. Savage, D. Faircloth, C. Gabor, S. Lawrie, A. Letchford, J. Bermejo, J. Lucas, J. Alonso, *et al.*, “Commissioning of the low energy beam transport,” *MOPEC078, Proceedings of IPAC*, vol. 10, 2010.
- [5] B. Biswas, “Spherical aberration from trajectories in real and hard-edge solenoid fields,” *Pramana*, vol. 86, no. 6, pp. 1299–1306, 2016.
- [6] J. D. Jackson, *Classical electrodynamics*. John Wiley & Sons, 2007.
- [7] A. Galejs and P. Rose, “Optics of electrostatic accelerator tubes, in septier, a (ed.): Focusing of charged particles, vol. ii,” 1967.
- [8] R. Baartman, “Quadrupole shapes,” *Phys Rev Special Topics Accelerators and Beams*, vol. 15, pp. 074002–074011, 2012.
- [9] R. Baartman, “Intrinsic third order aberrations in electrostatic and magnetic quadrupoles,” in *Proc. Particle Accelerator Conference, 1997*, vol. 2, pp. 1415–1417, IEEE, 1997.
- [10] R. Baartman, “Quadrupoles, to third order,” *arXiv preprint arXiv:1508.01576*, 2015.
- [11] R. Baartman, “End effects of beam transport elements,” *Talk at Snowmass, 2001*. Available at <http://lin12.triumf.ca/text/Talks/2001Snowmass/FF.pdf>.
- [12] C. Bovet, R. Gouiran, K. H. Reich, and I. Gumowski, “A selection of formulae and data useful for the design of ag synchrotrons,” tech. rep., CERN, 1970.
- [13] W. H. Press, B. P. Flannery, S. A. Teukolsky, W. T. Vetterling, *et al.*, *Numerical recipes*. Cambridge University Press, Cambridge, 1996.
- [14] E. Heighway and R. Hutcheon, “TRANSOPTR – a second order beam transport design code with optimization and constraints,” *Nuclear Instruments and Methods in Physics Research*, vol. 187, no. 1, pp. 89–95, 1981.
- [15] F. J. Sacherer, “RMS envelope equations with space charge,” *IEEE Transactions on Nuclear Science*, vol. 18, no. 3, pp. 1105–1107, 1971.
- [16] M. deJong and E. Heighway, “A first order space charge option for TRANSOPTR,” *IEEE Transactions on Nuclear Science*, vol. 30, no. 4, pp. 2666–2668, 1983.
- [17] I. Kapchinskij and V. Vladimirkij, “Limitations Of Proton Beam Current In A Strong Focusing Linear Accelerator Associated With The Beam Space Charge,” in *Proceedings, 2nd International Conference on High-Energy Accelerators and Instrumentation, HEACC 1959: CERN, Geneva, Switzerland, September 14-19, 1959*, pp. 274–287, 1959.

- [18] D. Edwards and L. Teng, “Parametrization of linear coupled motion in periodic systems,” *IEEE Transactions on nuclear science*, vol. 20, no. 3, pp. 885–888, 1973.
- [19] M. D’yachkov, R. Baartman, and F. Jones, “Multiturn simulation of coherent betatron resonance with space charge,” in *Particle Accelerator Conference, 2001. PAC 2001. Proceedings of the 2001*, vol. 1, pp. 267–269, IEEE, 2001.
- [20] K. L. Brown, F. Rothacker, D. C. Carey, and F. C. Iselin, “Transport: a computer program for designing charged-particle beam-transport systems,” Tech. Rep. SLAC-R-91-REV-3, Stanford Linear Accelerator Center, Calif., 1980.
- [21] K. Brown, D. Carey, C. Iselin, and F. Rothacker, “Technical report slac-75, cern 73-16, slac-91,” tech. rep., CERN-80-4, CERN, FNAL, SLAC, 1972.
- [22] K. Crandall, “TRACE3D documentation,” Tech. Rep. LAUR-90-4146, Los Alamos Accelerator Code Group, 1990.
- [23] M. Berz, “Computational aspects of optics design and simulation: COSY INFINITY,” *Nucl. Instrum. Methods*, vol. 298, pp. 473–479, 1990.
- [24] A. J. Dragt, R. D. Ryne, D. R. Douglas, F. Neri, C. T. Mottershead, E. Forest, L. M. Healy, P. Schütt, and J. van Zeijts, “Marylie 3.0 user’s manual,” *Department of Physics and Astronomy, University of Maryland, College Park, MD 20742-4111*, 1999.
- [25] R. Baartman, “TRANSOPTR Reference Manual,” Tech. Rep. TRI-BN-22-08, TRIUMF, 2022.
- [26] E. Chambers, “Particle motion in a standing wave linear accelerator,” in *Proc. 1968 Summer Study Superconducting devices and accelerators*, p. 79, Brookhaven National Laboratory, 1968.
- [27] R. Baartman, “Fast envelope tracking for space charge dominated injectors,” in *28th Linear Accelerator Conf.(LINAC’16), East Lansing, MI, USA, 25-30 September 2016*, pp. 1017–1021, JACOW, Geneva, Switzerland, 2017.
- [28] O. Shelbaya, R. Baartman, and O. Kester, “Fast radio frequency quadrupole envelope computation for model based beam tuning,” *Physical Review Accelerators and Beams*, vol. 22, no. 11, p. 114602, 2019.
- [29] T. P. Wangler, *RF Linear Accelerators*. John Wiley & Sons, 2008.
- [30] J. W. Staples, “Rfqsan introduction,” in *AIP Conference Proceedings*, pp. 1483–1532, AIP, 1992.
- [31] R. Baartman, “Fast envelope tracking for space charge dominated injectors,” in *Proceedings of LINAC 2016 Conference*, pp. 1017–21, 2016.
- [32] H. Goldstein, C. Poole, and J. Safko, *Classical Mechanics*. Addison Wesley, 2002.

- [33] M. De Jong and E. Heighway, "A first order space charge option for TRAN-SOPTR," *IEEE Trans. Nucl. Sci.*, vol. 30, no. 4, pp. 2666–2668, 1983.